Quaternary Science Reviews 198 (2018) 208–225

Contents lists available at ScienceDirect

Quaternary Science Reviews

journal homepage: www.elsevier.com/locate/quascirev

Holocene climatic and environmental evolution on the southwestern Iberian Peninsula: A high-resolution multi-proxy study from Lake Medina (Cádiz, SW Spain)

Tabea Schröder [a, *], Jasmijn van't Hoff [b], José Antonio López-Sáez [c], Finn Viehberg [b], Martin Melles [b], Klaus Reicherter [a]

[a] Institute of Neotectonics & Natural Hazards, RWTH Aachen University, Germany
[b] Institute of Geology & Mineralogy, University of Cologne, Germany
[c] Research Group Archaeobiology, Institute of History, CSIC, Madrid, Spain

ARTICLE INFO

Article history:
Received 8 May 2018
Received in revised form
3 August 2018
Accepted 30 August 2018
Available online 11 September 2018

Keywords:
Holocene
Palaeoclimatology
Western Europe
Mediterranean
Sedimentology
Lakes
Multi-proxy study

ABSTRACT

The climatic and environmental history of the SW Iberian Peninsula is explored to fill in the gap of continental palaeoclimate data by a high-resolution study of Lake Medina sediments from core Co1313. A multi-proxy approach comprising sedimentary facies analysis, elemental geochemistry, mineralogy, palynology and micropaleontology was employed to reconstruct the complex limnological response to climate change and catchment dynamics since the early Holocene. The further definition of abrupt climate change events was supported by a robust age model and rapid sediment accumulation rate at the study site. Proxies indicate arid and warm climate conditions during the Early Holocene, from around 9.5 to 7.8 cal ka BP, with a desiccation event at 8.8 cal ka BP as well as tentative evidence for the regional expression of a cold and abrupt arid climate event centering on ca. 8.2 cal ka BP. The Holocene Climate Optimum, from around 7.8 to 5.5 cal ka BP, is characterized by a humid climate and maximum lake level. Anoxic bottom water conditions are indicated by the preservation of sediment laminae and the occurrences of Sulfur mottles, which were observed for the first time within Holocene sediments of saline lakes. Mid-to Late Holocene times are governed by the 4.2 cal ka BP dry event as well as progressive aridification accompanied by the development of typical Mediterranean low-land vegetation. During recent times, further progressive loss in precipitation as well as fluctuating but overall increasing anthropogenic influence on Lake Medina sediments is observed.

1. Introduction

The western Mediterranean region, one of the most sensitive regions to climate change due to pronounced seasonal contrasts and its peculiar location at a climatic boundary (Lionello et al., 2006; Jiménez-Moreno et al., 2015), is predicted to be warmer and drier in future times (Giorgi and Lionello, 2008; Met Office et al., 2011). As a consequence a northward extension of arid lands is expected during the next decades (IPCC, 2014). Total consumption of ground water in Spain exceeds the annual input by 163%, reflecting a clear overuse of the aquifers (Puigdefábregas and Mendizabal, 1998). Predictions of future developments, however, are hampered by an insufficient understanding of past relationships between climate, vegetation history and human land-use (MET Office et al., 2011; Jiménez-Moreno et al., 2015).

The restricted knowledge of the Holocene climatic and environmental history in southern Spain is a consequence of discontinuous terrestrial climate archives (Roberts et al., 2008). The few archives available that cover the entire Holocene do suffer either from restricted age control or palaeoenvironmental sensitivity (Carrión et al., 2001, 2010; Reed et al., 2001; Fletcher et al., 2007; Schröder et al., 2017). In addition, only a few studies in continental Iberia show necessary chronological control for identification of short-term climate fluctuation (Ortiz et al., 2004) and most of them are located in elevated areas such as the Sierra Nevada (Anderson et al., 2011; Jiménez-Moreno et al., 2015; Ramos-Román et al., 2016, 2018). Moreover, multiple studies deal with a large variance of proxies, making a data combination or comparison difficult. Even

* Corresponding author.
E-mail address: tabea.schroeder@rwth-aachen.de (T. Schröder).

https://doi.org/10.1016/j.quascirev.2018.08.030
0277-3791/

more, the indices do differ in climate response times (Fritz and Anderson, 2013; Lane et al., 2013) and the interference of proxies with the ecosystem is complex (Birks and Birks, 2006). Our knowledge about Holocene climate history on land is mainly based on information from distal marine sediment cores (Combourieu Nebout et al., 1998, 2002; 2009; Voelker et al., 2006, 2009; Voelker and De Abreu, 2013) which are often of low temporal resolution (Fletcher et al., 2010).

Among the promising archives for investigating the climatic and environmental history of the southern Iberian Peninsula (IP) are sedimentary records from small and shallow endorheic lakes. These sediments are usually highly sensitive to the smallest climatic changes (Reed et al., 2001; Valero-Garcés et al., 2006; Martín-Puertas et al., 2010, 2011; Moreno et al., 2012), for instance, changing amounts of precipitation directly lead to strong variation in lake level and brine concentration (Fritz, 1996; Beklioglu et al., 2007; Davis and Stevenson, 2007).

Lake Medina (36°37′04``N, 6°03′13``W, 16 m a.s.l, Fig. 1) constitutes a low-lying, small, shallow and endorheic salt lake, located in the province of Cádiz within the Atlantic region of Andalusia (López-Sáez et al., 2002). A 10 m sediment core composite was previously retrieved in 1993 by Reed et al. (2001), showing that limnic sediments were continuously deposited in Lake Medina during the last 9.0 cal ka BP. This record was investigated for diatoms, ostracods, foraminifera, molluscs, aquatic pollen as well as lithology. Furthermore, the lake was investigated for stable isotopes by Roberts et al. (2008).

This study is based on a new high-resolution core composite of 25.7 m length that was obtained within the central part of the lake during two coring campaigns in 2014 and 2015. This study presents a multi-proxy approach applied to the Co1313 core, involving sedimentological, mineralogical, geochemical and palaeoecological methods to gain a detailed understanding of changes of the lake system over time and, by inference, Holocene climate change. Due to its exceptionally high temporal resolution, the record reflects not only long-term, millennial-scale climatic and environmental changes, but offers the possibility for comparison to also short-term, centennial-scale events from around 9.5 cal ka BP onwards.

2. Regional setting

Lake Medina is the second largest playa lake in the region of Andalusia in southern Spain (De Vicente et al., 2012) (Fig. 1 c, red star), located within the thermomediterranean bioclimatic belt (Quézel and Médail, 2003). Since the Ramsar Convention in 1989, the lake is part of a protected Nature Reserve (Fig. 1 d), declared as a Wetland of International Importance (De Vicente et al., 2012), even though lake water was recently used for irrigation. Lake Medina today is surrounded by agricultural land dominated by orchards of olive trees and cultivation of cereals and sunflower (Reed et al.,

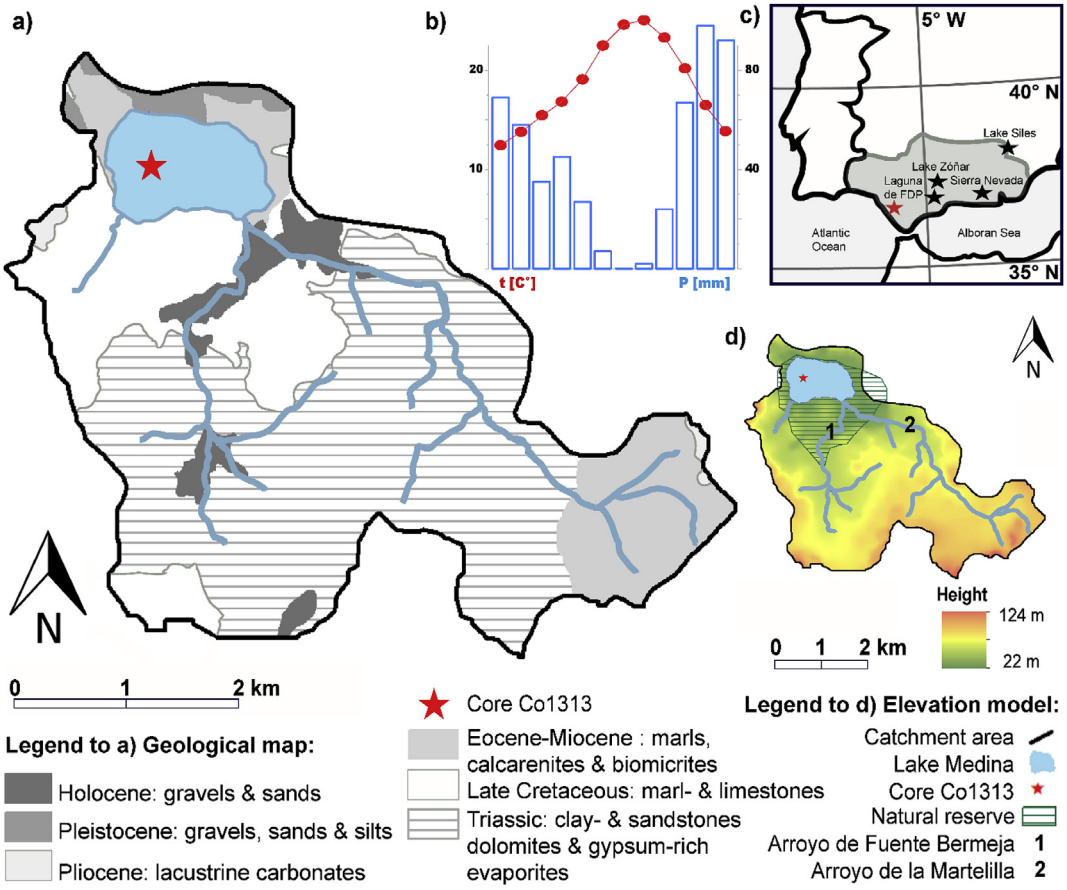

Fig. 1. a) Geological map of the catchment area of Lake Medina, b) Average monthly temperature T [C°] [displayed by red dots] and average monthly rainfall P [mm] [displayed in blue bars] from January to December measured at Cádiz between 1981 and 2010 (AEMET, Agencia Estatal de Meteorología), c) Overview map showing the location of the lake (red star) within the western Mediterranean and the region of Andalusia (in grey) on the southern Iberian Peninsula, together with some locations mentioned within the discussion, Lake Zóñar, Lake Siles, Laguna de Fuente de Piedra (FDP) and the Sierra Nevada, d) elevation model for the catchment area of Lake Medina also showing the area of the Natural Reserve, the location of the core Co1313 and the major temporal inlets (for names see legend). (For interpretation of the references to colour in this figure legend, the reader is referred to the Web version of this article.)

2001; Rodríguez-Rodríguez et al., 2012).

The endorheic lake is characterized by its semi-permanent, warm, polymictic and saline state (De Vicente et al., 2012; Fernández-Palacios, 1990) and surface and catchment areas of 1.2 km^2 and 16 km^2 respectively (Reed et al., 2001). Today, the maximum lake level amounts to 3.5 m, which is limited artificially by an overflowing ditch (Rodríguez-Rodríguez et al., 2012). The semi-permanent state of the lake is governed by desiccation in very dry years, related to the influence of the Mediterranean climate and the strong seasonality of temperature and rainfall (Bolle, 2003); the winter season is mild temperate and wet, and the summer time is hot and dry. Maximum precipitation occurs in autumn and winter (De Vicente et al., 2012; Magri et al., 2004) (Fig. 1 b). The mean annual precipitation amounts to 523 mm/yr and the mean temperature is 18.6 °C (Agencia Estatal de Meteorología). Main wind direction at the Lake Medina is SE and W (De Vicente et al., 2012), varying with alternating seasons and the position of atmospheric circulation patterns like the Azores High (Fletcher and Sánchez et al., 2008; Souza and Albuquerque Cavalcanti, 2009). On a decadal scale, the climate of southern Spain is influenced by the position of the North Atlantic Oscillation, being negative in wet seasons and positive in dry ones (Luterbacher et al., 2006).

The geology of the surroundings of Lake Medina is dominated by Triassic claystones and evaporites as well as by alluvial terraces built of Pleistocene sandstones and conglomerates in the eastern and northern area (Fig. 1 a). The Mediterranean soil layer *'capas rojas'* (Late Cretaceous) lies within the southern part, and mostly Tertiary clay- and marlstones and calcarenites in the west (IGME, 1982). The rocks and sediments of Tertiary and Triassic age are prone to halokinetic deformation (Wolf et al., 2014). Related to tectonic activity in the Gulf of Cádiz, diapiric uplift started in Miocene times (Medialdea et al., 2009). Due to the following lowered ground water level below the karst base, karstic erosion took place, which led to sinkhole formation (Rodríguez-Vidal et al., 1993; Valero-Garcés et al., 2014) and the formation of the lake basin in the Late Pleistocene (Rodríguez-Vidal et al., 1993). Today, clastic sediments are mainly supplied to the lake via the biggest temporary inlet, Arroyo de Fuente Bermeja, which enters the lake from the southeast, or via the smaller Fuente de la Martelilla to the southwest (van t Hoff et al., 2016) (Fig. 1 d) or by physical superficial erosion of the catchment.

The lake water salinity and lake level changes related to evaporation are not necessarily linked to each other (Reed et al., 2001), due to an interdependency of groundwater and infiltrated rocks of evaporitic origin within the lake catchment. The supply of saline ground-water may result in gypsum precipitation and accumulate saline lake water (Hardie et al., 1978; Reed et al., 2001; van t Hoff et al., 2016), even though the amount of ground-water entering the lake is regarded as being low, due to little permeable underground in the surroundings (Fernández-Palacios, 1990).

3. Materials and methods

The core composite Co1313 was retrieved from the same location within the deepest part of the lake during two coring campaigns in September 2014 and March 2015, from water depths of 1.7 and 3.2 m, respectively. The different water depth prevailed at the same site related to the different coring season. The core composite was constructed from correlation of up to 3 m long core sections, which were recovered with a gravity and percussion piston corer (UWITEC Corp. Austria). The core sections were cut into meter sections and stored dark, dry and cold until further processed at the laboratory of the University of Cologne.

Cores were opened lengthwise, described and photographed. Logging for magnetic susceptibility (MS) was performed with a Multi-Sensor Core Logger (GeoTek, 1 cm resolution). The MS data together with sedimentological and optical properties, were used for the correlation of overlapping core segments. Following this, the core composite was scanned for chemical composition with an X-Ray Fluorescence scanner (ITRAX, COX Analytical Systems; 2 mm resolution; exposure time 10 s, Cr tubes set to 50 kV and 38 mA). The data obtained were smoothed using a 19-pt running mean to reduce noise in the dataset.

Subsampling of the composite core took place at intervals of 6 cm (overall 427 samples). The bulk sediment subsamples were freeze-dried in order to exclude transformation of gypsum ($CaSO_4 \cdot 2H_2O$) to bassanite ($CaSO_4 \cdot 0.5H_2O$) or anhydrite ($CaSO_4$). Subsequently, the sub samples were split into aliquots for different measurements.

For geochemical analysis, all respective sample aliquots were ground to <63 μm to enlarge the surface area. For the analyses of total inorganic carbon (TIC) and total organic carbon (TOC), aliquots of ca. 35 mg were mixed with 10 g distilled water and measured with a Dimatoc 2000 (Dimatec Corp.). The contents of total nitrogen (TN) and total sulfur (TS) were measured on parallel sample aliquots of 5 mg with a vario Micro cube (Elementar Corp.).

Grain-size measurements were performed only on every 4th subsample (107 samples, interval of 24 cm), following treatment with 10 ml $NaCO_3$ (60 °C, 18 h), 10 ml 10% HCl (50 °C, 3 h), 5 ml 30% H_2O_2 (50 °C, 18 h), and 5 ml 1 M NaOH (90 °C, twice30 min) in order to remove the gypsum, carbonate, organic matter, and biogenic silica, respectively. Between these preparative steps, the samples were centrifuged and neutralized with deionized water. Prior to the measurements, the samples were mixed with $Na_4P_2O_7$ (0.05%) and shaken (>12 h) to avoid flocculation of clay minerals. Each sample was measured triply in 116 classes in a range between 0.04 and 2000 μm using a Laser Particle Size Analyser LS 13320 (Beckman Coulter Corp.) and the Frauenhofer optical model. The grain-size distributions were calculated using the program GRADISTAT (Blott and Pye, 2001).

For the mineralogical and elemental powder analyses, 111 aliquots of the ground samples were taken. Bulk mineralogical contents were determined by X-ray diffraction (XRD) on powder pellets using a diffractometer Bruker D8 Discover with Cu tube ($\lambda = 1.5418$ A, 40 kV, 30 mA) and the detector LYNXE_XE (opening angle = 2.9464°). The spectrum from 5° to 90° was measured in 4155 steps of 1 s exposure time. The evaluation of the spectra to minerals was computed using Match! (Crystal Impact (2014), Bonn, Germany, and SEARCH (Stoe and Cie (2003), Darmstadt, Germany) based on pdf2 (ICDD, 2003; Philadelphia, USA). The concentration of the minerals was evaluated using TOPAS Rietveld (Coelho, 2003), the same aliquot was scanned on the XRF scanner (1 mm resolution, exp. time of 60 s) using a Cr-tube (settings: 50 kV, 38 mA) for relative element intensities to statistically evaluate the elemental and mineralogical data using a principal component analysis (PCA) conducted with PAST software (Hammer et al., 2001). The outcome of the PCA plots within the 95% confidence interval.

The freeze-dried samples for ostracod analysis (ca. 5.0–12.4 g) were submerged in water and solidly frozen (−20 °C) overnight before they were carefully wet-sieved (63 μm mesh size). The residue was again freeze-dried and scanned under a stereomicroscope (magnification 64-fold). Complete carapaces were counted as two shells, broken shells more than 50% preserved were counted as a single shell. The taxonomy and ecological interpretation followed the studies by Meisch (2000), Mezquita et al. (2005) and Rasouli et al. (2016). The ostracod species were classified by their salinity preferences (<0.5 practical salinity unit (PSU) freshwater species; 0.5–5.0 PSU mesohalophilic species; > 5.0 PSU polyhalophilic species). Further, the ostracod record was assessed to identify objective intervals by a constrained hierarchical cluster analysis

(HCA), and used to reconstruct past host water conductivity based on the weighted average ecological preferences of Iberian ostracod species (Mezquita et al., 2005). The existing ostracod record investigated by Reed et al. (2001) was numerically treated similarly to compare both sedimentary records. A Gaussian LOESS filter was applied to the inferred conductivity data to smooth the results within a 95% confidence interval. All numerical calculations, and analyses were completed with the software package R (version 3.2.5) including the libraries Rioja and Vegan (R Core Team, 2013).

Pollen samples were taken at intervals of 24 cm (overall 100). The chemical preparation used for the extraction of pollen, spores and non-pollen palynomorphs was done with the addition of *Lycopodium* spores, by the use of 10% HCl (90 °C, 10 min), 15% KOH (90 °C, 10 min), sieving (mesh size of 112 μm), 40% HF (24 h), acetolysis (acetic acid treatment followed by acetic anhydrite and sulfuric acid (9:1), 90 °C, 10 min) and ultrasonic treatment, to remove carbonates, humic acids, coarse detritus and silicates, respectively. All steps were followed by neutralization with deionized water and centrifuging. Lastly, the residues of the samples were suspended in glycerine and sealed with glass and wax. Pollen samples were counted at the University of Aachen to minimum pollen sum of 300 (magnification 400-fold). Pollen and spore taxonomy mainly follows Beug (2004) and Reille (1992), further comparison was performed by the use of the modern reference collection of the CSIC in Madrid, Spain. Pollen and non-pollen palynomorphs diagrams were constructed using Tilia 2.0.41. Pollen zones were identified according to CONISS cluster analysis, included as well in Tilia 2.0.41 (Grimm, 1992). Hydro- and hygrophytic pollen taxa as well as non-pollen palynomorphs were excluded from the pollen sum and are represented with respect to the total pollen sum. Most pollen taxa displayed in Fig. 6 are grouped, which is related to their belongings and their significance as climate indicators. Charcoal was counted in parallel smaller and larger than 125 μm, both fractions are displayed in percent within the diagram of pollen and NPP's.

Chronostratigraphic information was obtained by radiocarbon measurements of 20 samples. Radiocarbon dating was performed on plant material of terrestrial origin in order to avoid falsification by reservoir effects of aquatic carbon (which is expected to highly influence the water plants of Lake Medina due to the surrounding karstic environment). Sample preparation followed a modified protocol of Rethemeyer et al. (2013). ^{14}C content was measured on a 6 MV Tandetron AMS (HVE, The Netherlands) at the University of Cologne (Dewald et al., 2013) and on a NEC compact model 0.5 MV AMS at the ^{14}CHRONO Centre at Queen's University Belfast (UBA). The ^{14}C dates were calibrated with OxCal v. 4.2 (Ramsey, 2009) using the INT-Cal13 curve (Reimer et al., 2013). The software package Bacon 2.2 (Blaauw and Christen, 2011) and implementation in the software R (R Core Team, 2013) was used to construct the depth-age model, overall stable sedimentation rates (mem. strength = 6, mem. mean = 0.7, thick = 10 cm) and expected sedimentation rates (acc. shape = 1.5, acc. mean = 4) were considered.

4. Results and discussion

4.1. Chronology

In southern Spain, most of the lakes are shallow saline water bodies (<0.50 m), which are characterized by significant natural fluctuations in water level driven by a five months summer water deficit and the irregular precipitation patterns of the Mediterranean climate (Álvarez Cobelas et al., 2005; Peel et al., 2007). This results in desiccation during arid years, leading to sediment hiatuses and organic matter (OM) preservation problems. OM may even be absent in shallow lakes with annual desiccation events such as Laguna Salada (close to the city of Campillos; Schröder et al., 2017). Lake Medina only dries out in exceptionally arid years, leading to relatively good preservation of OM. Such conditions enabled dating of terrestrial OM, bypassing the reservoir effect. Furthermore, previous studies faced difficulties with radiocarbon dating of bulk organic material in carbonate-rich areas because of the hard water effect (e.g. Björck and Wohlfarth, 2012; Höbig et al., 2016).

The age-depth model (Fig. 2) of Lake Medina is based on 20 ^{14}C dates on organic remains and provides a chronology for the last around 9.5 k years (Table 1). Except for three dates (UBA-32743, COL3423, and COL3291), the calibrated dates provide a mostly systematic sequence. The $\delta^{13}C$ values are in the range of −48.3 to −12.9‰, although most of the samples range between −25 and −20‰, suggesting the organic material being of terrestrial origin (Meyers and Ishiwatari, 1993).

The resulting age/depth succession (Fig. 2) is bracketed by a few

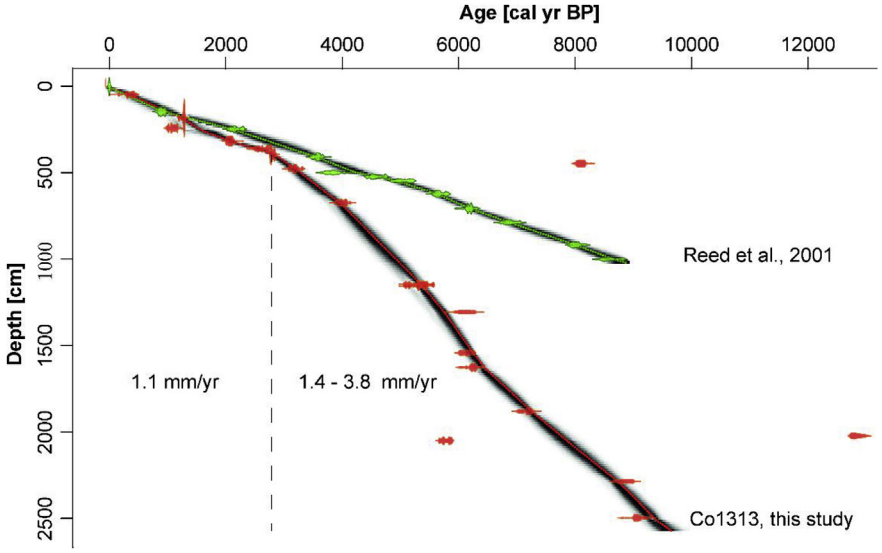

Fig. 2. Age depth model for Lake Medina. The orange ages represent this study, applied on core Co1313, the green ages reflect the ages by Reed et al. (2001). (For interpretation of the references to colour in this figure legend, the reader is referred to the Web version of this article.)

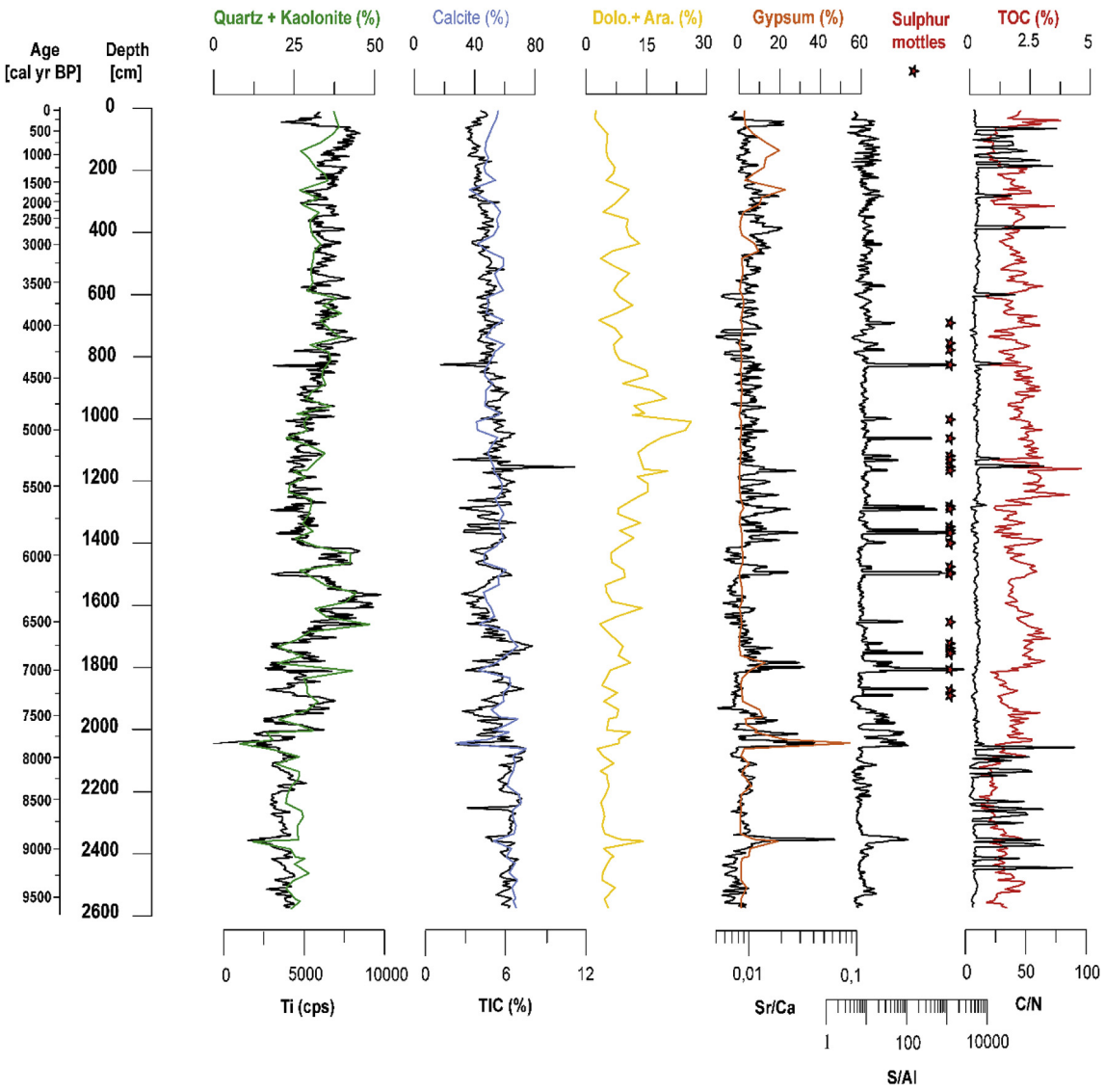

Fig. 3. Selected mineralogical and geochemical data of Co1313.

^{14}C ages, which obviously are erroneous. This includes samples UBA-32746 (242–244 cm depth) and COL3291 (2048–2050 cm), which represent too young ages in the order of 100 and 2000 yrs respectively. The small deviation of UBA-32746 might be related to bioturbation and penetration of roots (Kaland et al., 1984; Walker, 2005; Björck and Wohlfarth, 2012). The larger error of COL3291 might be due to contamination by younger bacteria or humic acids, because the piece of wood was not bleached properly during the preparation, comparable to a dating errors of a study performed on sediments in western Norway (Kaland et al., 1984). Too old ages are found in the samples UBA-32743 (447–449 cm), COL3417 (1303–1307 cm), and COL3423 (2020–2022 cm). The larger deviations from the age-depth model might represent the input of reworked organic material and thus could hint on periods of increased catchment erosion (Nambudiri et al., 1980; MacDonald et al., 1991).

The depth-age model of core CO1313 partly differs from the age-depth model of a core from a different location in Lake Medina, which was studied for diatoms, pollen, ostracods and δ^{18}O of ostracods by Reed et al. (2001). The data correspond well in the upper ca 4.5 m (since around 2.8 cal ka BP), suggesting relatively constant sedimentation rates of ca. 1.1 mm/yr. Below that depth (and age), sedimentation rates in the core investigated by Reed et al. (2001) were similar, whereas in core Co1313 they were much larger, in the order of 3.8 mm/yr. This might be related to the positions of the drill holes, the one of Reed et al. (2001) presumably closer located to the shore line.

The changes of the sedimentation rate and resulting lowered temporal resolution towards the top did not lead to subsequent sampling, which is related to the applied sampling procedure explained before, but also to elevated bioturbation within the upper meters (see Fig. 7).

4.2. Geochemistry, mineralogy, MS, grain-size and PCA

The sediments are dominated by calcite (50–70%), kaolinite (10–20%) and quartz (10–20%), some layers are enriched in gypsum (up to 50%), forming light, coarse-grained layers. In addition, minor occurrences of dolomite, aragonite, pyrite, halite, muscovite and clay minerals were detected. Variations in the MS coincide with changes of quartz and kaolinite concentration, as well as Ti, Rb, Fe, K, Al and Si, show an increased fluctuation between 20.50 and

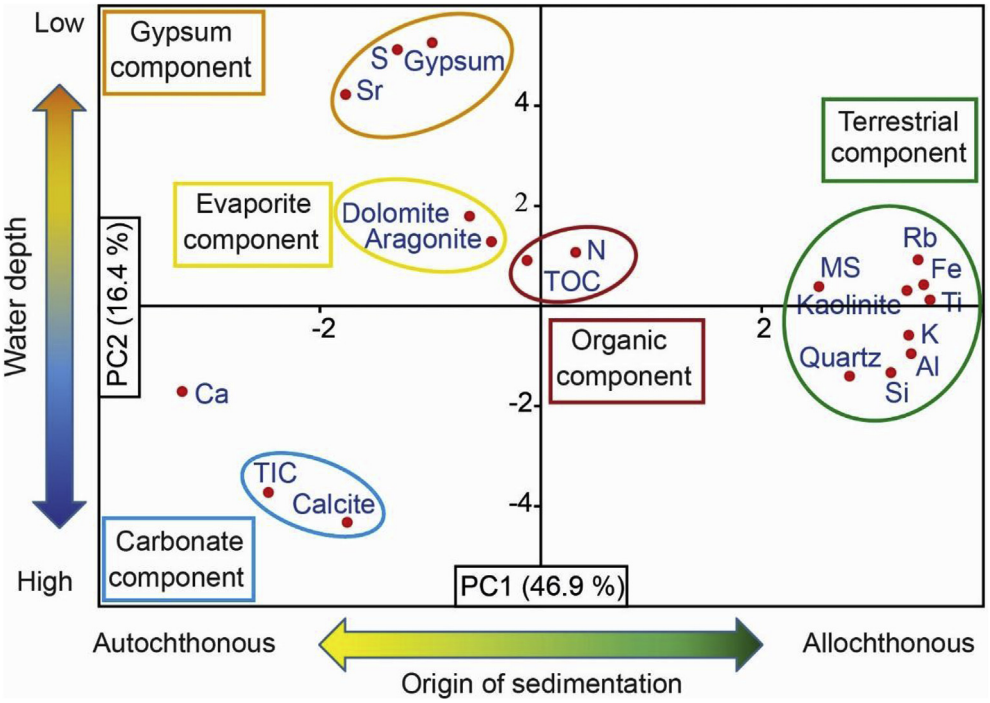

Fig. 4. PCA outcome and interpretation of geochemical, mineralogical and magnetic susceptibility data of Co1313 core. Arrows of water depth and origin of sedimentation indicate PCA axes interpretation.

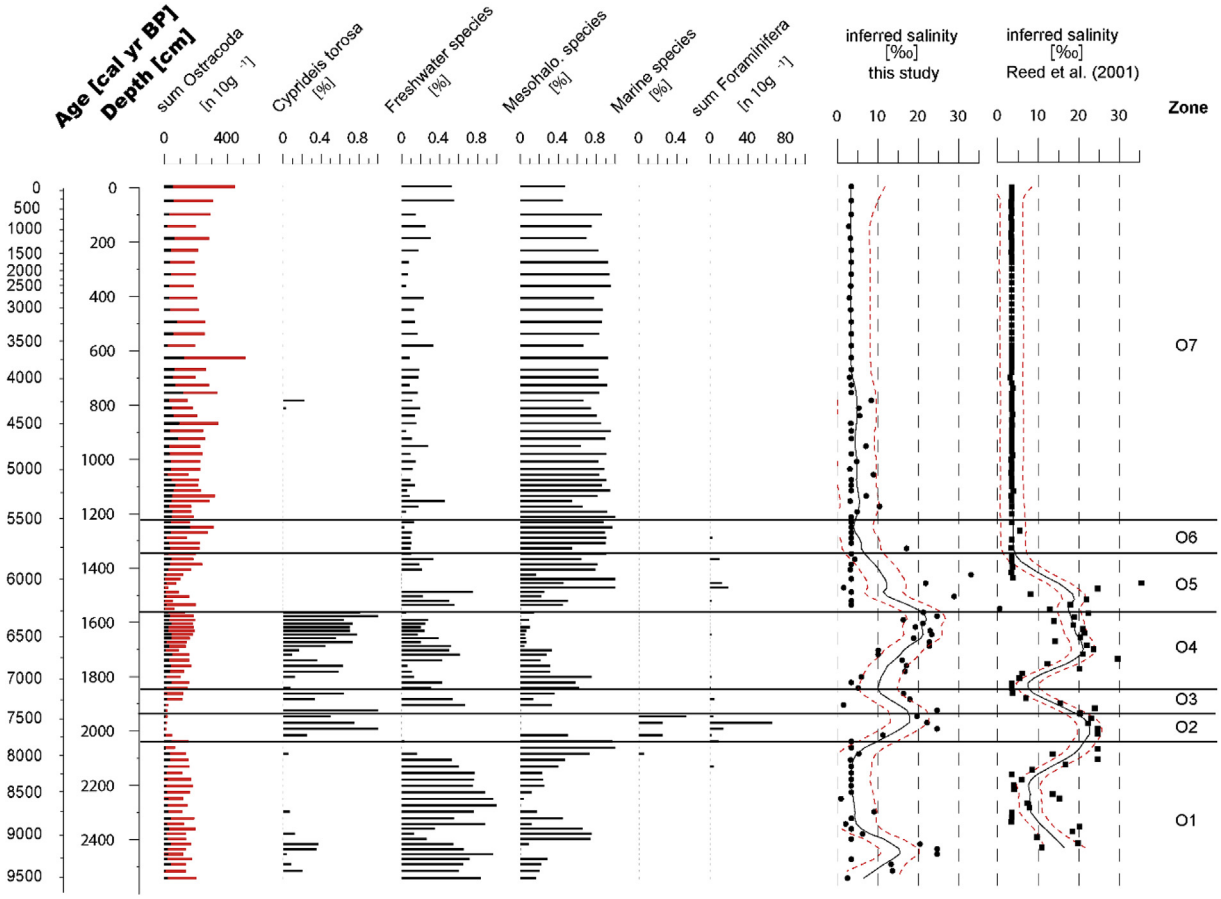

Fig. 5. Sum of total abundance of adult (red bars within sum Ostracoda) and juvenile (black bars) ostracods [n 10 g-1], and relative abundance of ostracod assemblages (Cyprideis torosa, freshwater species, mesohalophilic species, polyhalophilic species [%], and absolute abundance of Foraminifera [n 10 g-1]), as well as the calculated inferred salinity of core Co1313 and the study of Reed et al. (2001) [‰] and the ostracod zones O1–O7. (For interpretation of the references to colour in this figure legend, the reader is referred to the Web version of this article.)

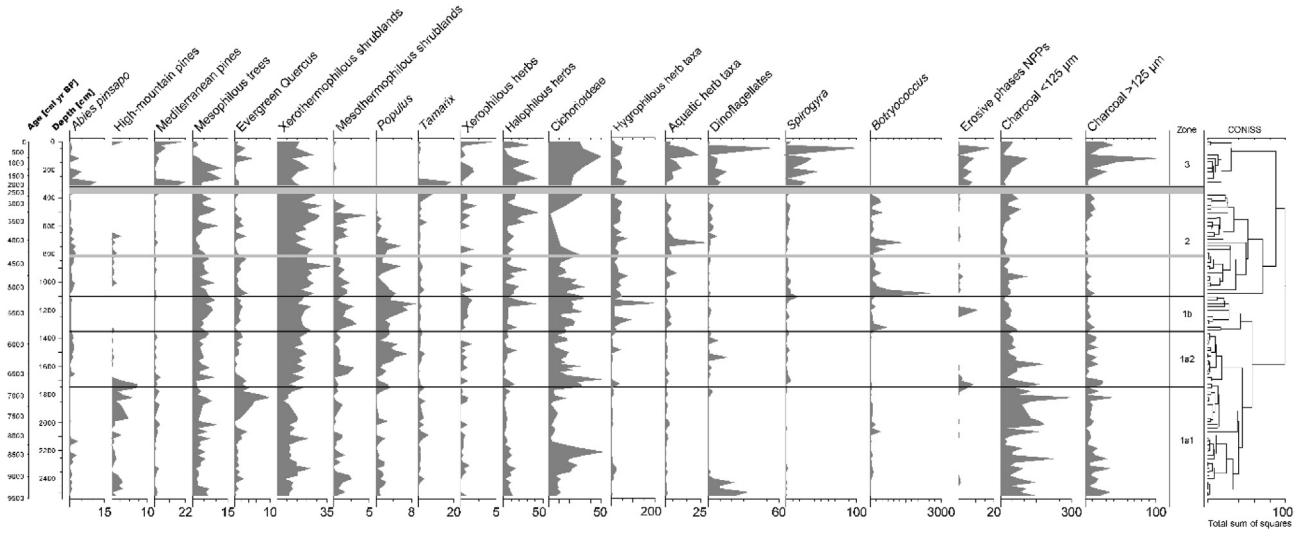

Fig. 6. Diagram of pollen, NPP's and charcoal particles [%] of the core Co1313 of Lake Medina. Ecological groups: High-mountain pines: Pinus sylvestris/nigra type; Mediterranean pines: *Pinus pinaster*, Pinus halepensis pinea type; Mesophilous trees: deciduous Quercus, Tilia, Corylus and Juglans; Xerothermophilous shrublands: Olea europaea, Phillyrea, Juniperus type, Pistacia lentiscus, Cytisus/Genista type, Cistus ladanifer type, Smilax aspera, Erica arborea type, Rubia peregrina type, Araceae, Daphne gnidium type, Rhamnus type; Mesothermophilous shrublands: Prunus type, Sambucus nigra-type, Arbutus unedo, Cistus populifolius-type, Lonicera, Viburnum, Hedera helix; Xerophilous herbs: Artemisia, Armeria/Limonium, Resedaceae, Helianthemum type; Halophilous herbs: Chenopodiaceae; Hygrophilous herbs: Phragmites, Cyperaceae; Typha latifolia type; Aquatic herbs: Ranunculaceae, Nuphar luteum type, Potamogetonaceae, Myriophyllum verticillatum type, Myriophyllum spicatum type, Hydrocharidaceae, Ruppia; Non-pollen palynomorphs (NPPs) indicators of erosive phases: Glomus.

Table 1
Results of AMS radiocarbon measurements on organic remains of core Co1313 from Lake Medina.

Lab sample no.	Depth (cm)	Age BP (yr) uncalibrated	± (yr)	Age BP (yr) calibrated	± (yr)	$\delta^{13}C$ (‰)
COL3288	48–50	287	44	362	62	−36.8
UBA-32745	183–185	1345	24	1247	60	−15.7
UBA-32746	242–244	1160	29	1080	98	−20.9
UBA-32747	317–319	2098	26	2069	70	−16.0
COL3412	360–364	2537	43	2621	131	−21.2
UBA-32748	394–396	2694	25	2803	46	−18.4
UBA-32743	447–449	7291	52	8091	106	−23.0
UBA-32744	477–479	2998	33	3201	130	−20.7
COL3413	672–676	3669	42	4017	130	−20.5
COL3414	1144–1146	4573	46	5250	199	−22.8
COL3415	1146–1151	4675	46	5446	134	−15.9
COL3416	1154–1156	4586	45	5257	203	−16.8
COL3417	1303–1307	5341	104	6113	201	−48.3
COL3419	1540–1542	5351	45	6138	138	−24.6
COL3420	1624–1626	5450	59	6212	187	−24.8
COL3421	1878–1880	6253	55	7141	139	−21.4
COL3423	2020–2022	10967	63	12858	141	−23.9
COL3291	2048–2050	5023	40	5777	117	−28.2
COL3425	2283–2285	8001	61	8832	184	−21.1
COL3427	2493–2497	8128	53	9128	142	−12.9

14.00 m depth (around 7.8–5.9 cal ka BP, Fig. 3). The Sr/Ca ratio matches the variability of gypsum in the lower core part very well, with highest intensities in the laminated sediments, as well as in the upper part of the record, which are rather homogeneous and bioturbated. S/Al reveals maxima where sulfur mottles occur and represents the gypsum component. The latter reflects periods of gypsum precipitation due to a low lake level or entire desiccation (Roca and Julià, 1997). TIC follows the trend of calcite occurrence and decreases upwards in contrary to TOC values. The C/N ratio fluctuates above 17 up to 20.5 m depth, followed by stable but lower values below 7 up to 6 m depth (and approximately 3.5 cal ka BP) and increased but unsteady values (>15%) towards the top (Fig. 3).

The principal component analysis (PCA) (Fig. 4) shows a clustering of geochemical and mineralogical proxies and explains their dependency relationship (Hammer et al., 2001). Five sediment components were defined, reflecting the depositional environment and processes of sedimentation. PC1 shows differences of endogenic sedimentation through gypsum, other evaporites and carbonate components on the negative side (calcite, dolomite, aragonite and gypsum, elements Ca, Sr, S as well as TIC). The terrestrial component, shown by various indicators for allochthonous sedimentation (like MS, quartz and kaolinite as well as Rb, Fe, Ti, K, Al and Si), is shown on the positive side. PC1 therefore reflects changes between allochthonous and autochthonous sediment supply. The endogenic sedimentation is indicative for (highly) concentrated shallow to desiccated environments, whereas high lake levels coincide with a high influence of terrestrial components like the elements iron or titanium or the mineral quartz (Giralt and Julià, 2003; Boës et al., 2011; Martín-Puertas et al., 2011) due to

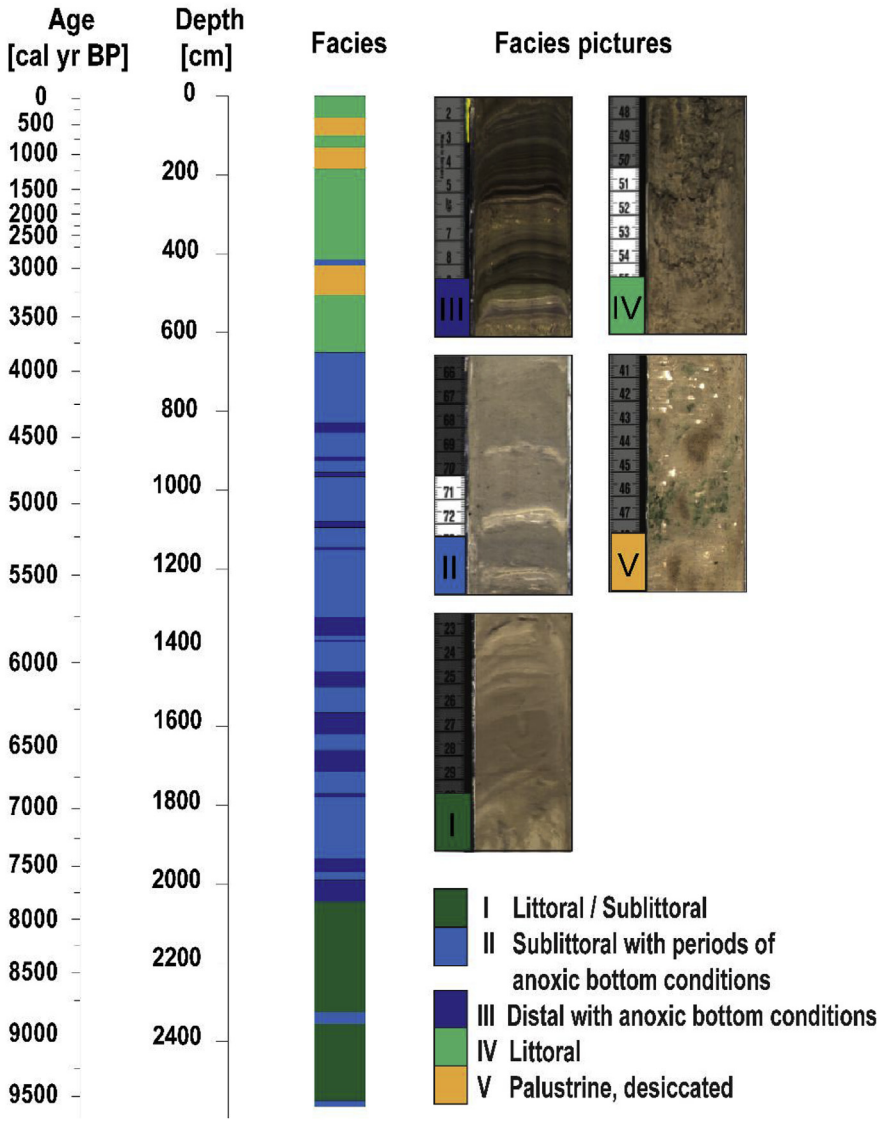

Fig. 7. Facies of Co1313 together with exemplary pictures of the sedimentary facies and the interpretation of the depositional environment.

enhanced soil erosion related to precipitation (López et al., 2006; Jiménez-Espejo et al., 2008; Martín-Puertas et al., 2010, 2011; Ramos-Román et al., 2018). In addition, the terrestrial input is indicative for the presence of an active inlet (Renaut and Gierlowski-Kordesch, 2010). At Lake Medina, the Arroyo de Fuente Bermejo is the main deliverer for terrestrial material (van t Hoff et al., 2016). However, a significant change of grain-size is not noted during phases of increased terrestrial input and the influence of wind on sedimentational processes can be neglected. Modern sedimentation patterns indicate a limited influence of coarse-grained sediments within the first 200 m from the shore line (van t Hoff et al., 2016). Grain-size analysis detected a 90% domination of a fraction below 16 μm and overall little variation is observed. Sand was detected only between 20.5 and 19.5 m depth.

The PC2 reflects changes of water level, which might be excessive in these shallow lake settings through irregular precipitation patterns (Álvarez Cobelas et al., 2005). The typical evaporitic sequence evolved out of evaporation and concentration processes (Giralt and Julià, 2003) is clearly reflected within the Lake Medina sediments through precipitation of carbonates, sulphates and chlorides (positive loadings of PC2, namely gypsum, dolomite, aragonite as well as the elements S and Sr). Within an evaporitic lake sequence, the first precipitates are calcite and aragonite, the latter being more soluble than the former one. The presence of dolomite is likely related to primary precipitation within this sabkah-like environment but might also be related to dolomitization of aragonite, linked to an increased Mg/Ca ratio due to gypsum precipitation (Tucker and Wright, 1990). Gypsum will be deposited within the next chemical precipitation step, its occurrence within Lake Medina is largely controlled by the dissolution of the Triassic subsurface within the catchment (IGME, 1982) and coincides with a shallow lake level with highly saline conditions of a desiccated lake with a gypsum crust (Stein et al., 1997). The high Sr intensities reinforces this assumption, since Sr exchanges with Ca in gypsum as salinity or evaporation increases (Santisteban et al., 2016). Therefore, Sr is often a good indicator for palaeosalinity, related to the exchange of Sr for Ca under saline conditions (Dodd and Crisp, 1982; Santisteban et al., 2016). If the water level increases thereafter, the efflorescent crusts may be easily dissolved (Tucker and Wright, 1990), which again increases salinity and precipitation of aragonite and dolomite (Vegas et al., 2010). Further refilling phases with fresh water are reflected by higher influence of terrestrial

material (loadings around zero on PCA axis 2; MS, quartz and kaolinite as well as the elements Rb, Fe, Ti, K, Al and Si) as well as carbonate precipitation as observed in Lake Zóñar (Martín-Puertas et al., 2011). Ca (negative loading on PCA axis 2 together but distant from calcite and TIC) is usually a good indicator for the presence of inorganic carbonate, but it shows weak correlation with both TIC and calcite (coefficients of determination r^2 0.58 and 0.41 respectively) and indicates a more complex pattern of origin, for instance gypsum and dolomite.

The organic component is shown through increased presence of nitrogen in the bulk sediment and total organic carbon (TOC) within the lake sediments and clusters around zero. Elevated concentrations of TOC in Co1313 are interpreted as being deposited during anoxic periods of lake level high stands, because of the enhanced preservation of organic matter (OM) during times of low to zero oxygen level at the lake floor (Meyers and Lallier-Vergès, 1999).

The presence of sulfur is not only related to gypsum occurrence, but also to sulfur mottling, mainly occurring between 19 and 7 m depth (around 7.3 to 3.9 cal ka BP). The mottles displace the laminated sediments and consist of diagenetic elemental sulfur, which is comparable to findings within the sediments of Lake Lisan in Israel (Torfstein et al., 2008). It may form due to bacterial sulphate reduction during anoxic conditions in lakes with SO_4^{2-} concentrations below 100 μM (Rudd et al., 1986; Ziegenbalg et al., 2010). Dissolution of gypsum by precipitation and the supply of dissolved gypsum through ground water delivered SO_4^{2-} for microbial sulphate reduction. OM is oxidized by sulphate-reducing bacteria, which leads to production of reduced sulfur species (Feely and Kulp, 1957). This may take place in the lower water body of the stratified lake, or within the bottom sediments (Ziegenbalg et al., 2010). Highest concentrations of elemental sulfur are usually recovered in near-surface sediments (Urban et al., 1999). Therefore, it is likely that the mottles within Co1313 core were formed close to the water-sediment interface, indicating anoxic bottom conditions at times of deposition. Hydrogen sulphide is either abiologically or biologically oxidized to native sulfur, but the exact mechanisms are still unknown (Machel, 1992). In hypersaline lakes of Holocene age, accumulation of native sulfur was not yet detected (Ziegenbalg et al., 2010; Lindtke et al., 2011).

4.3. Palaeobiology

4.3.1. Ostracods

A continuous ostracod record was discovered and in total, the fossil fauna holds 16 taxa (Table 2). All species are known to be halotolerant or halophilic (Athersuch et al., 1989; Meisch, 2000; Mezquita et al., 2005; Rasouli et al., 2016). Seven ostracod zones were identified by a constrained hierarchical cluster analysis of the relative abundance record (Fig. 5).

The first ostracod zone (O1; bottom to 20.40 m (around 7.8 cal ka BP) is characterized by a well-established freshwater (halotolerant) fauna with some influence of mesohalophilic species (Fig. 5). The following ostracod zone (O2; 20.40–19.44 m, around 7.8–7.4 cal ka BP) is dominated by mesohalophilic species, especially *Plesiocypridopsis newtoni*. The third ostracod zone (O3; 19.44–18.48 m, around 7.4–7.1 cal ka BP) holds polyhalophilic species including *Cyprideis torosa* and foraminifera species, i.e. *Ammonia beccarii,* which might reflect chloride dominated conditions (De Deckker and Lord, 2017). The next zone (O4; 18.48–15.60 m, around 7.1–6.2 cal ka BP) is a mix of freshwater species, here especially *Ilyocypris* sp. mesohalophilic species and the occurrence of polyhalophilic *C. torosa*. The succeeding species assemble of the adjacent zone (O5; 15.60–13.44 m, around 6.2–5.8 cal ka BP) is dominated by *C. torosa*, which is accompanied by mainly freshwater species and minor abundance of mesohalophilic species. Then a sharp transition occurs in the following ostracod zone (O6; 13.44–12.24 m, around 5.8–5.5 cal ka BP), as shells of *C. torosa* disappear and the species assemblages infer freshwater, mesohaline waters and only few periods of polyhaline conditions (i.e. *Eucypris mareotica*). The top most zone (O7; 12.24 m to top, around 5.5 cal ka BP to recent) comprises a stable domination of shells of mesohalophilic species and successively fading of singular occurrence of polyhalophilic species (i.e. *E. mareotica*). *C. torosa* has a final occurrence between 4.80 and 4.56 m depth (3–2.9 cal ka BP). The inferred salinity values (‰) derived by ecological preferences given in Mezquita et al. (2005) and the former study of Reed et al. (2001) show a very high comparability, even though the species composition within Co1313 is more diversified (Table 2).

The occurrence of foraminifera is sporadic and restricted to samples of the lower part of the core, *Ammonia beccarii* (Linnaeus, 1758) was the only species found within.

4.3.2. Pollen, non-pollen palynomorphs & charcoal

The results of pollen, non-pollen palynomorphs (NPPs) and charcoal analysis (>125 μm and <125 μm) are displayed (Fig. 6) together with five pollen assemblage zones (1a1, 1a2, 1b, 2 and 3). Four out of 100 samples (at 816, 360, 336 and 312 cm depth, displayed by grey horizontal bars within the pollen diagram), did not reach the envisaged counts of 300.

The first zone (1a1; bottom to 17.50 m, around 9.4 to 6.8 cal ka BP) is dominated by arboreal pollen of high-mountain pines. Moreover, there is a concordance of evergreen *Quercus* and the evolution of high-mountain pines between 19.5 and 17.50 m depth. Occurrence of halophilous herbs are low to moderate and fluctuate around 5%, while hygrophilous plants are present on a very low level. Dinoflagellates are present in the lowermost part of zone 1a1 with up to 35%. Both fractions of charcoal particles are highly fluctuating but abundant, apart from an interval at around 21.50 m depth. Until the same depth, Cichorioideae pollen are highly abundant and strongly lowered in the following. A general and close correlation of mesophytic taxa and charcoal particles, as found within the sediments of Lake Siles by Carrión (2002) may not be assured. The following pollen zone (1a2; 17.50–13.50 m; around 6.8–5.8 cal ka BP) shows higher values of riparian pollen taxa like *Populus* and a strong decrease in high-mountain pines, while halophilous taxa are represented on a low level. Charcoal particles show a decreasing trend, while xerothermophilous taxa show higher abundances in comparison to the previous pollen zone. The next zone (1b; 13.50–11.00 m; around 5.8–5.2 cal ka BP) shows higher values of mesothermophilous shrublands and higher appearances of halophilous herbs at the top, while charcoal particles decrease. The adjacent pollen zone (2; 11.00–3.25 m; 5.2–2.3 cal ka BP) reveals a sharp transition to modified nutrient conditions, shown by very high occurrences of *Botryococcus neglectus* (Jankovská and Komárek, 2000). Mesophilous trees are dominant, as well as xerothermophilous shrublands and pollen of aquatic herb taxa. Alluvial poplar forests are substituted after lowering by Tamarisk formations (*Tamarix*) in the upper part of zone 2. Overall, the increasing presence of Chenopodiaceae marks an increasing salinity of the soils surrounding the lake. The end of this zone as well as the beginning of the upper zone (3; 3.25 m to top, around 2.3 cal ka BP to recent) is marked by the non-presence of countable pollen sums, related to bad or even non-preservation of pollen grains. Charcoal values are very low and show a decreasing trend within these depths. Pollen zone 3 is characterized by mesophilous temperate and cool temperate summer-green trees, xerothermophilous shrublands and asynchronous occurrences of halophilous herbs and hygrophilous herb taxa. *Botryococcus* disappeared, while Dinoflagellates and *Spirogyra* get abundant at the expense of

Table 2
List of ostracod and foraminifera taxa of core Co1313 and comparison to the previous study from Reed et al. (2001). The calculated optimum conductivity (optiCOND) as given in Mezquita et al. (2005) is used to classify species in freshwater (0–1.5 mS cm-1), mesohalophilic (1.5–8.0 mS cm-1) and polyhalophilic (>8.0 mS cm-1) groups.

Taxa name Ostracods:	CO1313	Reed et al. (2001)	optiCOND [ms/cm]	group
Candona neglecta (Sars, 1887)	x	x	0.457	freshwater
Cyprideis torosa (Jones, 1850)	x		31.623	polyhalophilic (marine)
Cypris bispinosa (Lucas, 1849)	x		1.479	freshwater
Darwinula stevensoni (Brady and Robertson, 1870)	x	x	1.230	freshwater
Eucypris mareotica (Fischer, 1855)	x	x	48.978	polyhalophilic
Eucypris pigra (Fischer, 1851)	x		0.676	freshwater
Herpetocypris intermedia (Kaufmann, 1900)	x		0.891	freshwater
Heterocypris incongruens (Ramdohr, 1808)			1.148	freshwater
Heterocypris salina (Brady, 1868)	x	x	2.089	mesohalophilic
Ilyocypris sp. 1	x	x	1.023	freshwater
Leptocythere sp. 1			NA	polyhalophilic (marine)
Limnocythere inopinata (Baird, 1843)	x		2.455	mesohalophilic
Loxoconcha elliptica (Brady, 1868)	x		19.953	polyhalophilic (marine)
Plesiocypridopsis newtoni (Brady and Robertson, 1870)	x	x	5.128	mesohalophilic
Sarcypridopsis aculeata (Costa, 1847)	x		7.943	mesohalophilic
Trajancypris clavata (Baird, 1838)	x		1.660	mesohalophilic
Foraminifera: *Ammonia beccarii* (Linnaeus, 1758)	x	x	NA	

Chenopodiaceae. The endemic species of *Abies pinsapo* occur in high percentages at the onset of pollen zone 3.

4.4. Sedimentology and facies interpretation

The first facies I (Fig. 7) identified (25.5–20.45 m depth, around 9.5–7.8 cal ka BP) consists of massive carbonate-rich clayey to silty sediments undisturbed by bioturbation. It is interpreted as littoral to sublittoral facies reflecting a period of fluctuating moderate to high lake level, supported by e.g. fluctuating conductivity (Fig. 5) related to catchment erosion of the Triassic evaporites through run-off (Reed et al., 2001) and the alternating but overall high C/N ratio (Fig. 3). These peaks of C/N values points towards pulses of terrestrial organic matter within the lake environment (Meyers and Ishiwatari, 1993; Meyers, 1994, 1997; 2003; Meyers and Lallier-Vergès, 1999; Cohen, 2003), probably due to enhanced fluvial supply from the Arroyo de Fuente Bermejo (van t Hoff et al., 2016) or surficial catchment run-off. The great amount of carbonate suggests a relatively high water table as a consequence of enhanced weathering of adjacent marls and limestones within the catchment area; karstic solution and sinkhole evolution as well as lake basin formation should also be considered.

Facies II, which interrupts the first facies twice, is build up by massive clayey and carbonate-rich silts. It likely reflects a rather humid period, with fluctuating but moderate to high salinity values related to increased catchment erosion, shown by the alternation of deposition of massive clayey silts during shallower phases and laminated sediments during phases with a high water column (Reed, 1996; Eusterhues et al., 2005; Valero-Garcés et al., 2014). The terrestrial component is modest and points towards moderate fluvial input or catchment erosion related to moderate precipitation. Moreover, diagenetic sulfur mottles indicate anoxic bottom conditions (Ziegenbalg et al., 2010).

The second facies alternating with the third facies (being progressively dominant towards the top), consists of gypsum and carbonate layers (0.5–2 cm thick). The first occurrence of facies III at 20.45 m depth (at around 7.8 cal ka BP) marks a significant transition within the sedimentary record from massive homogeneous towards highly laminated sediments with mm-scaled gypsum and carbonate layers. Coarse grained layered sediments consist of gypsum. Facies III represents time periods of humid climate with maximum lake level, shown by high salinity values related to increased terrestrial input and anoxic bottom conditions, characterized by the occurrence of finely laminated sediments (Valero-Garcés et al., 2014). Therefore it is interpreted as distal facies with anoxic conditions. TOC is highest during this period, also pointing towards a high water level and anoxic bottom conditions, able to preserve the organic matter (Meyers and Lallier-Vergès, 1999; Meyers, 2003) and enhanced fluvial supply. The carbonate content is relatively high, related to predominant influence of terrestrial components. The gypsum sedimentation is generally low, while some peaks do indicate dry events and highly concentrated lake water (Martín-Puertas et al., 2011). The low gypsum occurrence also points towards a high lake level, as it disables the gypsum precipitation, despite the high salinity of the lake water (Torfstein et al., 2008). In addition, white mottles of 80–90% elemental sulfur indicating anoxic conditions (Rudd et al., 1986; Ziegenbalg et al., 2010) and high water level can be found (Fig. 2) within alternating facies II and III. The alternating massive and laminated sediments of these facies, and the interpretation of changes between moderate to high water level and variation between mixed and stratified lake water (governed by water depth; stratification is limited by a water column of 6 m (Shaw et al., 2004)) is comparable to other Spanish lakes such as Lake Areo (Corella et al., 2010) or Lake Zóñar (Martín-Puertas et al., 2009, 2011).

From 6.51 m (around 3.7 cal ka BP) towards the top, little laminated, rather homogeneous and bioturbated facies IV and V occur. Lithofacies IV is build up by massive carbonate-rich clayey silts while similar facies V consists of massive carbonate-rich clayey silts incorporating 1–3 mm white and/or 1–5 mm green mottles of carbonates and gypsum. Facies IV points towards a rather arid climate and shallow lake level, indicated by traces of bioturbation such as roots (Cohen, 2003; Valero-Garcés et al., 2014) pointing towards a littoral depositional environment. Gypsum deposition is relatively low, while the evaporite component in terms of dolomite and aragonite deposition is dominant, interrupted by an increased carbonate and terrestrial component, indicating some periods of lake filling after desiccation. Furthermore, the C/N ratio within facies IV is low, revealing a lacustrine origin of the organic matter (Meyers and Ishiwatari, 1993; Meyers, 1994, 1997; 2003; Meyers and Lallier-Vergès, 1999; Cohen, 2003).

Facies V reflects very shallow waters and periods of lake water desiccation, shown e.g. by strong bioturbation (Valero-Garcés et al., 2014) and high gypsum deposition. The calcite content is decreasing upwards, reflecting a lowering lake level. Additionally,

high C/N peaks indicate enhanced terrestrial organic influence (Meyers and Ishiwatari, 1993; Meyers, 1994, 1997; 2003; Meyers and Lallier-Vergès, 1999; Cohen, 2003), maybe related to increasing aerial input and influence instead of elevated catchment erosion through precipitation as the terrestrial component in general is low, indicating a low energy regime and little alluvial input (Valero-Garcés et al., 2014). The depositional environment during sedimentation of facies V is interpreted as being littoral and palustrine to desiccated.

4.5. Palaeoclimatic significance

4.5.1. Early holocene (around 9.5–7.8 cal ka BP)

The beginning of the record in the Early Holocene is characterized by the presence of open land indicators which indicate a warm and rather arid climate (Burjachs et al., 2016; Langgut et al., 2014) together with the occurrence of *Pinus halepensis pinea* type (classified as Mediterranean pine within Fig. 6) (López-Sáez et al., 2010, 2009). It most likely reflects the time after lake basin evolution, when the lake presumably had steep margins and an irregular lake bed, suggested by e.g. the high sedimentation rate and the sedimentary facies. The water depth presumably was relatively low to moderate and the depositional environment of Co1313 was littoral to sublittoral with rapid fluctuations of salinity (Figs. 4 and 8), indicated by the succession of the ostracod species *P. newtoni*, *C. torosa*, *D. stevensoni* and *Ilyocypris sp.* until around 9 cal ka BP (Table 2). The interpretation of shallow-to moderate water depth and rapid fluctuations in salinity are in accordance to the record of Reed et al. (2001). Variation in C/N ratio (Fig. 3) is likewise inferred as an alternation between lacustrine and terrestrial origin of OM (Meyers, 1997) and repeated pulses of the former into Lake Medina.

A prominent desiccation event likely occurred at around 8.8 cal ka BP, evidenced by gypsum precipitation and lowered terrestrial components as well as slightly postponed higher values of xerophilous and xerothermophilous plant taxa, likely indicating relatively dry conditions (Jalut et al., 1997; Carrión, 2002; Glais et al., 2017) (Fig. 8). The change of plant taxa occurrences within Co1313 might reflect changes in moisture availability rather than temperature (Osborne et al., 2000; Jalut et al., 2009). These findings on the Early Holocene climate of the southern Iberian Peninsula prior to around 8 cal ka BP confirm other studies in the region, which also concluded a warm climate with arid conditions during this period (Pantaléon-Cano et al., 2003; Fletcher et al., 2007; Schneider et al., 2016). This was related to low evaporation of seawater caused by relatively low sea surface temperatures producing less humidity and less rainfall amount in this region (Cacho et al., 2002) (Fig. 8), obviously in concordance to our multi-proxy based data. Mauri et al. (2015) described the Early Holocene in the southern IP as being 2 °C colder than present, but with fluctuating temperature conditions.

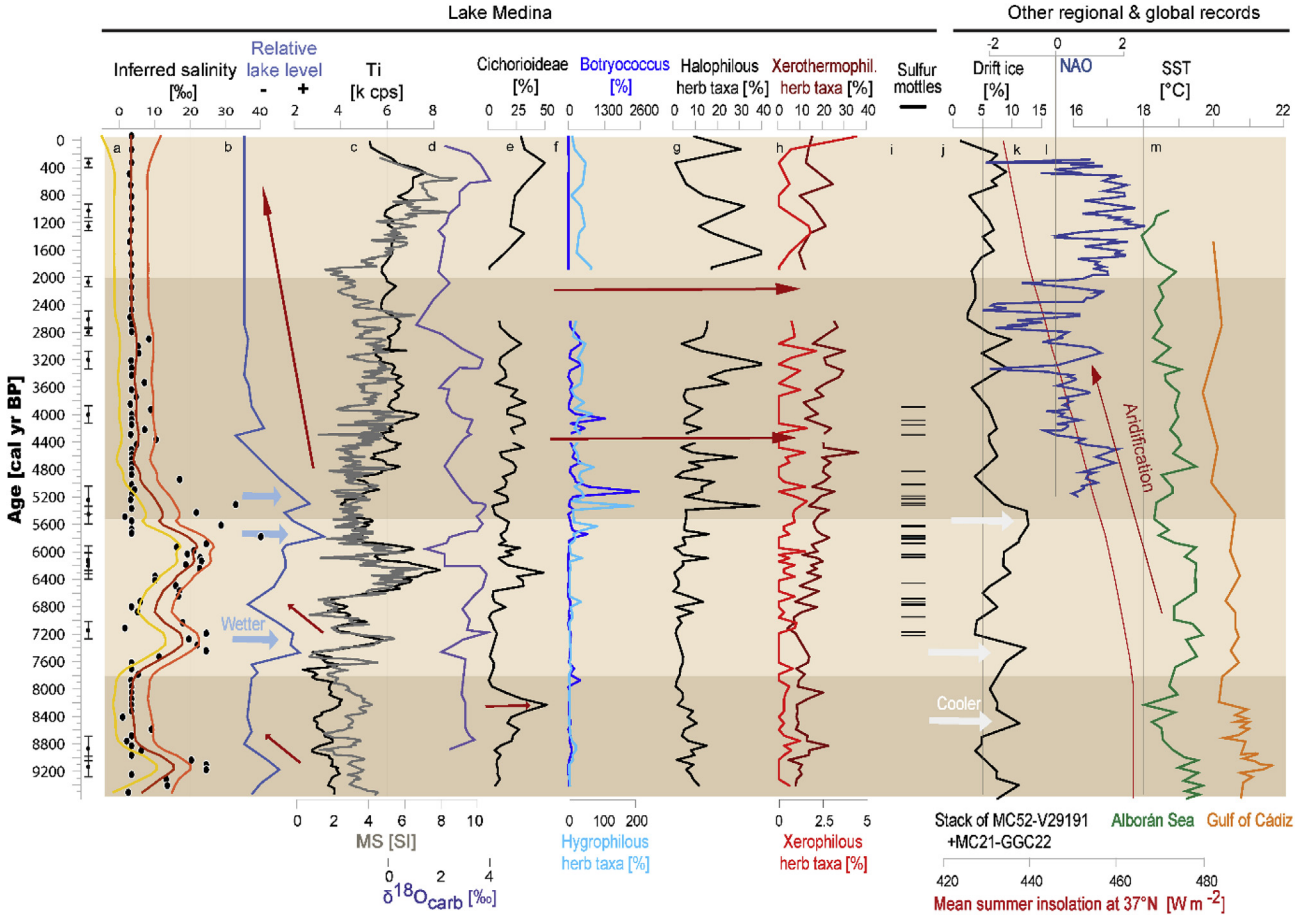

Fig. 8. *From left to right: Age scale [cal yr BP] and tie points of AMS ^{14}C dates (with error bars) as well as an overview of the most relevant indices of Lake Medina: a) the inferred salinity [‰], b) the inferred relative lake level, c) the terrestrial input displayed by the titanium [cps] and MS curve, d) the $\delta^{18}O_{carb}$ record (Roberts et al., 2008) of Lake Medina, e) Cichorioideae, f) Botryococcus & hygrophilous herb taxa, g) halophilous herb taxa, h) xerothermophilous- and xerophilous herb taxa, i) occurrence of sulfur mottles. Other regional and global records are displayed by j) the drift ice index inferred by a stack of 4 records (Bond, 2001), k) the mean summer insolation for 37° N (Hodell et al., 2015), l) NAO index (Olsen et al., 2012) and m) the sea surface temperatures in the Alborán Sea and the Gulf of Cádiz (Cacho et al., 2002). Red arrows indicate aridification, light blue arrow illustrate increased humidity, and white arrows points at times of increased coldness.* (For interpretation of the references to colour in this figure legend, the reader is referred to the Web version of this article.)

During the Early Holocene, a short period has been recognized between ca. 8.2–7.8 cal ka BP, coinciding with the Bond 5b event and related melt water outbursts freshening the North Atlantic, when cool and arid conditions governed most of the Northern Hemisphere (Bond et al., 1997; Bond, 2001; Mayewski et al., 2004; Alley and Ágústsdóttir, 2005). In southern Spain, it was identified as period of arid and cold conditions (Combourieu Nebout et al., 2009; Jiménez-Espejo et al., 2007, 2008; López de Pablo and Jochim, 2010). By `colder' conditions, a decrease of roughly 1 °C was quantified by previous studies (Davis et al., 2003). The 8.2 cal ka BP event is not widely registered in palaeoclimate records of the Mediterranean, maybe related to the scarcity of high-resolution records or uncertainties and imprecision in dating (Alley and Ágústsdóttir, 2005; Davis and Stevenson, 2007; Morellón et al., 2009). Within Co1313 data, the 8.2 cal ka BP event might be characterized by decreasing terrestrial influence and low salinity (inferred by lowered catchment erosion of the surrounding Triassic evaporites) (Fig. 8). However, it has to be said that the age model does not anchor the 8.2 event to a performed dating measurement and that the event as well as its timing have to be interpreted with caution. The increase of xerophilous and xerophytic taxa like Cichorioideae at around 8.25 cal ka BP can be interpreted as a drier episode. Towards 8 cal ka BP, the percentages hit a low, indicating moister conditions together with slightly higher occurrences of mesophilous taxa. However, high gypsum precipitation points towards a desiccation event at around 8 cal ka BP, but the ostracod data show no response. Charcoal particles hit a low towards 8 cal ka BP which indicates lowered available biomass at this time (Linstädter and Zielhofer, 2010; Riera Mora et al., 2004; Swetnam and Betancourt, 1990). Moreover, plants require (variable) time for migration as answer to climate change (Huntley, 1991) and it remains questionable to what extent a rapid shift in temperature or precipitation exerts an influence on vegetation. Alley and Ágústsdóttir (2005) however postulated major changes within the vegetation patterns related to the 8.2 cal ka BP event, even though it lasted only a few decades.

4.5.2. Holocene climate optimum (7.8–5.5 cal ka BP)

The so-called Holocene Climate Optimum (HCO) was a warm and humid period in the SW Mediterranean (Carrión, 2001; Jalut et al., 2009; Anderson et al., 2011; Magny et al., 2012; Walker et al., 2012; Fletcher and Zielhofer, 2013), also concluded by Roberts et al. (2008) and Reed et al. (2001) from the study of the other Lake Medina record. The HCO is related to summer insolation maxima (Laskar et al., 2004), which contributed to warming and an increase of the thermic land/sea contrast, thereby leading to an empowered wind generation and higher precipitation in fall and winter (Tuenter et al., 2003; Meijer and Tuenter, 2007). Main estuaries of the southwestern Iberia were inundated until around 7 cal ka BP due to sea-level rise (Boski et al., 2008). Within Co1313, the HCO is given distinction by the lamination of sediments and elevated influence of terrestrial components through catchment erosion by precipitation (Fig. 8, visible by Ti [cps] and MS [SI]; representatives of the allochthonous lake sediments, Fig. 4), comparable to e.g. Lake Estanya, N Spain (Morellón et al., 2009). Moreover, a large deviation of one dating sample (COL3423) lets suggest increased catchment erosion at the beginning of the HCO (MacDonald et al., 1991; Nambudiri et al., 1980). The dominance of both facies II and III indicate a period of maximum lake level above at least 6 m (Shaw et al., 2004) (Fig. 8). Diagenetic sulfur mottles reinforce this thesis, as they do indicate anoxic bottom water conditions (Ziegenbalg et al., 2010) (Fig. 8). Moreover, high values of charcoal indicate a high amount of biomass available for fire propagation and summer droughts during high annual variability of precipitation (Swetnam and Betancourt, 1990; Whelan, 1995; Riera Mora et al., 2004; Linstädter and Zielhofer, 2010; Ramos-Román et al., 2016). Mesophilous trees like e.g. *Populus nigra* became more frequent within the surroundings of Lake Medina, but a strong correlation of both charcoal and mesophilous trees, as seen in Lake Siles (Carrión, 2002), is not obvious. The increases of Cichorioideae pollen in comparison to the end of the Early Holocene period is now most likely not climate inferred, but related to its anthropogenic nitrophilous character (Abel-Schaad et al., 2018) and increasing human influence (T. Schroeder, unpublished). Elevated occurrences of evergreen *Quercus* towards around 7 cal ka BP strengthen the presumption of a humid climate through milder conditions (Jiménez-Moreno et al., 2013) in concordance to findings at the ODP Site 976 in the Alborán Sea (Combourieu Nebout et al., 2009). However the authors do also describe a substantial decrease in forest cover after 7 cal ka BP, which cannot be confirmed by the boreal pollen findings of Co1313 record.

A remarkable shift in ostracod assemblages (Table 2) occurs within this time period and shows a trend towards higher saline conditions, possibly due to enhanced catchment erosion. It is noteworthy that especially the first peak in salinity is inferred only by the dominant occurrence of *C. torosa* and simultaneous presence of *Leptocythere* sp. *Loxoconcha elliptica* and foraminiferas. Eventually, the absolute values of salinity are then based mainly on the salinity optimum of dominating *C. torosa*, which is known to have also a wide tolerance and capability of surviving much higher salinities (Neale, 1988). The sedimentation rate is very high within this time (Fig. 2; 3.5 mm/yr by contrast to other lakes as e.g. Lake Zóñar (1.5 mm/yr; around 150 km to the NE of Lake Medina (Fig. 1)) (Martín-Puertas et al., 2008, 2011), Lake Siles (0.08 mm/yr; approximately 370 km to the NE (Fig. 1)) (Carrión, 2002), Laguna de Fuente de Piedra (0.5 mm/yr; around 130 km to the NE (Fig. 1)) (Höbig et al., 2016), Lake Estanya (0.3–2.11 mm/yr, Northern Spain) (Morellón et al., 2009) or a peat bog in the Sierra Nevada (0.058 mm/yr; around 250 km to the NE (Fig. 1)) (Ramos-Román et al., 2018). Such high sedimentation rates can be found as well in estuarine environments after the rapid sea level rise, e.g. in the Guadiana estuary in Portugal (Fletcher et al., 2007). The high sedimentation rate of our record is likely caused by elevated carbonate precipitation during periods of high lake level, low sediment erosion due to the high water level and the hyperboloid form of the lake, resulting in sediment transport and final deposition from littoral to deeper areas (Davis, 1968; Lehman, 1975). Hygrophilous vegetation however shows very low occurrences, only interrupted by two peaks at around 6.8 and 6.2 cal ka BP, accompanied by the elevated appearance of halophilous taxa, maybe related to increased salt concentration within the surrounding soil and lake water (Glais et al., 2017; Prentice et al., 1996). The salinity of the Lake Medina water is related to the erosion of the surrounding Triassic evaporites through surface run-off, therefore the salinity likely increases in more humid times (Reed et al., 2001; van t Hoff et al., 2016). This inverse relationship is reinforced through the presence of Chenopodiaceae (halophilous herb taxa) in times of elevated precipitation, which is in contrast to other lake studies, where an increase indicate semi-desert climate conditions (Anderson et al., 2011; Burjachs et al., 2016; Fletcher and Sánchez et al., 2008; Langgut et al., 2014; López-Sáez et al., 2002). Reed et al. (2001) describes a time of maximum lake level between 6.9 and 6.6 cal ka BP (matching with the 6000 BP widespread humidity maximum) with gradual lake shallowing from 6.7 cal ka BP onwards, while our record shows an indication of maximum lake level (inferred by salinity, facies, sulfur occurrence, chemical composition etc.) between around 6.2 to 5.8 cal ka BP (Fig. 8) followed by gradual reduction. At around 6 cal ka BP, there is a negative peak within the stable isotope record, indicating chemically more dilute and less saline water in contrast to our new record of Lake Medina.

However, the isotope record is based only on individual values of ostracods within this depth, lowering the accurateness of information (Roberts et al., 2008).

4.5.3. Mid-to late holocene (5.5–2 cal ka BP)

The Mid-to Late Holocene is a period of progressive aridification, related to lowered solar output (Mayewski et al., 2004) and reduced summer insolation (Hodell et al., 2015) (Fig. 8) with a deferred onset on the IP (Fletcher and Zielhofer, 2013); e.g. being dated on southeastern Spain to around 5.9–5.5 cal ka BP (Carrión et al., 2003) and in northern Spain (Lake Estanya) from 4.8 cal ka BP onwards (Morellón et al., 2009).

Proxies of CO1313 indicate a decrease in terrestrial input until around 5.3 cal ka BP (Fig. 8) as well as a lowering of the salinity pointing towards drier conditions, interrupted by several periods of comparatively higher precipitation; in concordance to the first record obtained at Lake Medina. In general, lake water conditions in Lake Medina were brackish, shallow and temporally anoxic at the lake bottom, approved by the occurrence of diagenetic sulfur mottles (Ziegenbalg et al., 2010). In contrast to the HCO, when the terrestrial input parameters and the inferred salinity showed a close correlation, these proxies seem to be no longer closely related to each other. Elevated sediment input in consequence of increasing aridity might be responsible for such coherence (Sly, 1978) as well as displacements of the catchment area. Information concerning the temperatures during the Mid-to Late Holocene comes from xerothermophilous shrublands like *Olea europaea* and *Phillyrea,* indicating warm-temperate climate conditions. Moreover, the substitution of alluvial poplar forests by Tamarisk formations indicate a loss of precipitation. The lowered summer insolation, leading to cooling of the sea surface temperature (Fig. 8) and a decreasing land-sea temperature contrast that infers reduced precipitation, supports this interpretation of the climate.

At 5.3 cal ka BP there is a peak in the occurrence of hygrophilous taxa followed by a contemporary peak in halophilous herb taxa (Fig. 8), which might be related to decreasing salinity of the lake water. *Botryococcus* appearance shows several highs and reinforce the shallow and brackish water hypothesis mentioned for Mid-to Late Holocene times, relatively low rainfall and high seasonal variability (Guy-Ohlson, 1992; Batten and Grenfell, 1996). No evidence is found in the Co1313 record for the Holocene event at around 4.8 to 4.5 cal ka BP for showing elevated temperatures at the southern Iberia (Wanner et al., 2011). In northern Spain, Lake Estanya experienced shallower conditions related to increased evaporation from 4.8 cal ka BP onwards (Morellón et al., 2009).

The 4.2 cal ka BP event, also called Bond 3 event after Bond (2001), may have led to demographic migration in the southern Iberia from SW to SE regions (deMenocal, 2001; Brooks, 2012; Lillios et al., 2016) and cultural changes between the Copper and Bronze ages (López-Sáez et al., 2014; Lillios et al., 2016). This event might be detectable within our data through a low salinity and lowered lake water level from that time onwards (Fig. 8). Moreover a pollen gap related to very low preservation of organic matter, likely verifies a dry event at around 4.25 cal ka BP that had larger influence on the surroundings of Lake Medina as the former 8.2 cal ka BP climate event. The recent event is declared as one of the six periods of significant rapid climate change within Holocene times (Mayewski et al., 2004). An identification of three aridity pulses instead of one event at 4.2 cal ka BP, at around 4.5, 4.3 and 4.0 cal ka BP, as in the Sierra Nevada (Ramos-Román et al., 2018) based on decreases of TOC, *Botryococcus* and Mediterranean forests, is dissented by our findings, which rather point towards a gradual reduction in precipitation from around 4.2 cal ka BP onwards. Moreover, decadal to multi-century cyclicity of 170, 200, 240, 300, 680 and 800 years of climate variations, comparable to those described by Ramos-Román et al. (2018), were not identified.

The time between around 3.1 and 2.5 cal ka BP is known as a time of rapid climate change towards drier and colder conditions on most regions of the northern and southern hemisphere (Mayewski et al., 2004). For the SW Iberian Peninsula, an aridity crisis during the 3rd millennium cal BP is described by Martín-Puertas et al. (2010). In core Co1313, increased aridity is indicated by a facies shift suggesting more littoral conditions and a shift in pollen taxa (Figs. 5 and 8), likely related to lowered effective precipitation and colder conditions. However, Wanner et al. (2011) postulates no significant temperature changes for the southern Iberian Peninsula. From around 2.8 ka cal BP onwards, sedimentation rates of both records, the former study of Reed et al. (2001) and the new Co1313 core, are similar. Within our record, this time period is governed by very low to no pollen preservation, again likely related to oxidation of organic matter related to lowered lake level and periodic but quantitatively increased lake desiccation periods (Bennett and Willis, 2002; Carrión et al., 2009). This might have led to the establishment of similar depositional environments of both cores and equal sedimentation rates. The former Lake Medina record shows another negative peak of the isotope record at around 2.6 cal ka BP, which suggest less saline water (Roberts et al., 2008) in agreement with our record of Lake Medina.

4.5.4. Modern (<2 cal ka BP)

The beginning of this period coincides with the onset of the Iberian Roman Humid Period, the warmest period within the last 2000 years, which lasted until 1.5 cal ka BP (Borja et al., 1999; Martín-Puertas et al., 2009). In contrary to other studies of Lake Zoñar and Padul (the latter located at the Sierra Nevada) (Martín-Puertas et al., 2009; Jiménez-Moreno et al., 2013, 2015; Ramos-Román et al., 2016, 2018) and an indication towards a humid time period, our record is marked by an increase in xerophilous and anthropogenic nitrophilous taxa (Fig. 8 and T. Schröder, unpublished). This indicates drier and warmer conditions (as well as elevated human influence), comparable to other marine and lake studies (Corella et al., 2010; Moreno et al., 2012) and in agreement to the former Lake Medina study of Reed et al. (2001) as well as repeatedly positive NAO values (Olsen et al., 2012) (Fig. 8). Substitution of *Populus* by *Tamarix* indicates a progressing loss of precipitation (Langgut et al., 2014). Moreover, a gypsum peak as well as the facies interpretation and occurrence of evaporite mottles point towards a shallowing of the lake with periods of desiccation (Valero-Garcés et al., 2014) in facies V. The distinct increase in non-pollen palynomorphs like Dinoflagellates, *Spirogyra*, and *Glomus* as indicator for erosive phases (Fig. 8) (López-Merino et al., 2009) moreover points towards increased anthropogenic influence, e.g. through increasing grazing pressure and land use (López-Sáez and López-Merino, 2007; Ramos-Román et al., 2018). Surprisingly high percentages of *Abies pinsapo* (Spanish fir, based on the presumption of the regional representation of *Abies* in southern Spain, the morphotype of *Abies pinsapo* was assumed (Alba-Sánchez et al., 2010; Cortés-Sánchez et al., 2008)) represent regional growth in the surroundings of Lake Medina. This might be related to human influence; as today, it growths within the southwestern Baetic mountain range between 900 and 1800 m a.s.l. on the Iberian Peninsula.

The Medieval Climate Anomaly (MCA) between approximately 1.05 and 0.65 cal ka BP (Ramos-Román et al., 2016; Moreno et al., 2012; Martín-Puertas et al., 2009, 2010) is worth mentioning as it was an exceptional arid period in Iberia (Martín-Puertas et al., 2009, 2010; Morellón et al., 2009; Moreno et al., 2012; Ramos-Román et al., 2016, 2018) and the Alborán Sea (Nieto-Moreno et al., 2011). Our data shows confirmative increased deposition of

gypsum and aragonite as well as maxima of the C/N ratio (Fig. 3). However, Moreno et al. (2012) suggest rather humid climate conditions during the MCA at Atlantic ocean sides like Lake Medina. Within core Co1313, no laminations are preserved nor diagenetic sulfur spots, leading to the assumption of a lake level which was too low for deposition and preservation of laminated sediments as well as the generation of sulfur mottles. In addition, it was likely influenced by increasing bioturbation. Terrestrial input increases meanwhile, accompanied by charcoal sedimentation (Fig. 6), maybe related to higher aerial input, anthropogenic influence, as well as lake shallowing. A clear statement about vegetation history cannot be given due to low sampling resolution within this time period, related to pollen sampling in depth intervals instead of time steps. In addition, the ongoing bioturbation of sediments may have led to imprecise or erroneous interpretations of the climate and environment at specific points of time and was therefore omitted.

Other studies (Puigdefábregas and Mendizabal, 1998; Mayewski et al., 2004) and records, like that of Lake Zóñar (Martín-Puertas et al., 2008, 2010) or a peat bog at the Sierra Nevada mountain (Ramos-Román et al., 2016) point towards pronounced oscillations of precipitation within the last 0.7 cal ka BP and the cooler Little Ice Age. The same corresponds to Bond 0, described by Wanner et al. (2008) as coldest hemispheric multidecadal-multicentury long Holocene period since the 8.2 cal ka BP event, related to low orbital forcing of the Northern Hemisphere, decreased solar activity and frequent volcanic eruptions. However, climate conditions are more difficult to reconstruct from recent Co1313 sediments due to potential anthropogenic overprint, decreasing lake level already suggesting a drying climate and increasing bioturbation of the sediments, as well as lowered sample resolution. However, a strong increase in steppe/desert forbs as well as halophilous herbs and erosive phase NPP's clearly points towards a reduction in precipitation and risen salinization of the surrounding soils, affirmed by the former study of Reed et al. (2001), also postulating a trend towards shallowing of Lake Medina.

5. Conclusion

The multi-disciplinary research on the 25.7 m long sediment record Co1313 of Lake Medina, which comprises approximately the last 9.5 k years, has demonstrated that:

(1) The high-resolution sedimentary sequence of the endorheic saline Lake Medina offers the possibility to interpret and compare palaeoenvironmental changes, climatological history and lake evolution on a regional to global scale and fills in the gap of continental palaeoclimate data on the southern Iberian Peninsula, one of the most sensitive regions to climate change (Jiménez-Moreno et al., 2015; Lionello et al., 2006).

(2) A multi-disciplinary study which includes an interdisciplinary approach including sedimentology, geochemistry, mineralogy, biology and chronology is indispensable to give a wide overview and obtain as much information of the palaeoenvironment as possible, as the interplay of the various proxies with the environment is very complex (Birks and Birks, 2006).

(3) Comparison to the sedimentary record of Lake Medina obtained by Reed et al. (2001), additionally investigated for stable isotopes by Roberts et al. (2008), showed remarkable differences within e.g. the sedimentation rate before 2.8 cal ka BP and the preservation of organic matter, but also strong similarities, like the salinity and lake level interpretations. Therefore, lake studies concerning palaeoclimate and –environment need great understanding about the depositional environment and depositional processes and should be explored by multiple cores and studies of the lake surroundings.

(4) The study of pollen and ostracods has shown to be the most promising and constructive tool for the investigation of long-term climate evolution of Lake Medina from an arid and warm Early Holocene, to the humid Holocene Climatic Optimum, followed by progressive aridification from Mid-to Late Holocene times. Moreover, short-term climate events as e.g. the 8.2 cal ka BP event and the obviously more severe 4.2 cal ka BP climate event could have been identified and lake evolution and depositional processes were explored. However, detection of short-term climate events is limited by dating accuracy, sampling and measurement interval but also preservation of climate indices within the lake sediment.

(5) More research should be done with regard to the adaption to ongoing climate change, as recent data of sediment core Co1313 of Lake Medina point towards less precipitation in the region of SW Iberia, which might lead in the foreseeable future, together with water exploitation, ongoing soil salinization, –erosion and desertification, to complete desiccation of Lake Medina.

Acknowledgements

This article is a contribution to the project C1 within the CRC 806 'Our way to Europe', supported by the German Research Foundation (DFG). We like to thank the guards of the Nature Reserve for their support and hospitality, and the Junta de Andalucía for giving permission to work at Lake Medina. Special thanks goes to the drilling crew and Prof. Dr. F. Schäbitz of the University of Cologne for providing pollen lab facilities. We also thank the reviewers for their helpful comments and criticism.

References

Abel-Schaad, D., Iriarte, E., López-Sáez, J.A., Pérez-Díaz, S., Sabariego Ruiz, S., Cheddadi, R., Alba-Sánchez, F., 2018. Are *cedrus atlantica* forests in the rif mountains of Morocco heading towards local extinction? Holocene. https://doi.org/10.1177/0959683617752842, 095968361775284.

AEMET, Agencia Estatal de Meteorología, Ministerio de Agricultura y pesca, alimentación y medio ambiente (aemet.es; access on 28.February.2018).

Alba-Sánchez, F., López-Sáez, J.A., Benito de Pando, B., Linares, J.C., Nieto-Lugilde, D., López-Merino, L., 2010. Past and present potential distribution of the Iberian Abies species: a phytogeographic approach using fossil pollen data and species distribution models. Divers. Distrib. 16, 214–228.

Alley, R.B., Ágústsdóttir, A.M., 2005. The 8k event: cause and consequences of a major Holocene abrupt climate change. Quat. Sci. Rev. 24, 1123–1149.

Álvarez Cobelas, M., Rojo, C., Angeler, D.G., 2005. Mediterranean limnology: current status, gaps and the future. J. Limnol. 64, 13–29.

Anderson, R.S., Jiménez-Moreno, G., Carrión, J.S., Pérez-Martínez, C., 2011. Post-glacial history of alpine vegetation, fire, and climate from Laguna de Río Seco, Sierra Nevada, southern Spain. Quat. Sci. Rev. 30, 1615–1629.

Athersuch, J., Horne, D.J., Whittaker, J.E., 1989. Marine and brackish water ostracods. In: The Linnean Society of London & the Esturine and Brackish-water Sciences Association by E.J. Brill.

Batten, D.J., Grenfell, H.R., 1996. Green and blue-green algae. In: Jansonios, J., McGregor, D.C. (Eds.), Palynology: Principles and Applications. American Association of Stratigraphic Palynologists Foundation, pp. 205–214.

Beklioglu, M., Romo, S., Kagalou, I., Quintana, X., Bécares, E., 2007. State of the art in the functioning of shallow Mediterranean lakes: workshop conclusions. Hydrobiologia 584, 317–326.

Bennett, K.D., Willis, K.J., 2002. Pollen. In: Smol, J.P., Birks, H.J.B., Last, W.M. (Eds.), Tracking Environmental Change Using Lake Sediments.Volume 3: Terrestrial, Algal, and Siliceous Indicators. Kluwer academic publishers, pp. 5–32.

Beug, H.-J., 2004. Leifaden der Pollenbestimmung für Mitteleuropa und angrenzende Gebiete, first ed. Verlag Dr. Friedrich Pfeil München.

Birks, H.H., Birks, H.J.B., 2006. Multi-proxy studies in palaeolimnology. Veg. Hist. Archaeobotany 15, 235–251.

Björck, S., Wohlfarth, B., 2012. 14C chronostratigraphic techniques IN paleolimnology. In: Last, W.M., Smol, J.P. (Eds.), Tracking Environmental Change Using Lake Sediments. Kluwer Academic Publishers, pp. 557–578.

Blaauw, M., Christen, J.A., 2011. Flexible paleoclimate age-depth models using an autoregressive gamma process. Bayesian Anal 6, 457–474.

Blott, S.J., Pye, K., 2001. Gradistat: a grain size distribution and statistics package for the analysis of unconcolidated sediments. Earth Surf. Process. Landforms 26, 1237–1248. https://doi.org/10.1002/esp.261.
Boës, X., Rydberg, J., Martinez-Cortizas, A., Bindler, R., Renberg, I., 2011. Evaluation of conservative lithogenic elements (Ti, Zr, Al, and Rb) to study anthropogenic element enrichments in lake sediments. J. Paleolimnol. 46, 75–87.
Bolle, H.-J., 2003. Climate, climate variability, and impacts in the mediterranean area: an overview. In: Bolle, H.-J. (Ed.), Mediterranean Climate - Variability and Trends. Springer Verlag.
Bond, G., 2001. Persistent solar influence on North Atlantic climate during the Holocene. Science (80-.) 294, 2130–2136.
Bond, G., Showers, W., Cheseby, M., Lotti, R., Almasi, P., DeMenocal, P., Priore, P., Cullen, H., Hajdas, I., Bonani, G., 1997. A pervasive millennial-scale cycle in North Atlantic Holocene and glacial climates. Science (80-.) 278, 1257–1266.
Borja, F., Zazo, C., Dabrio, C.J., del Olmo, F.D., Goy, J.L., Lario, J., 1999. Holocene aeolian phases and human settlements along the Atlantic coast of southern Spain. Holocene 9, 333–339.
Boski, T., Camacho, S., Moura, D., Fletcher, W., Wilamowski, A., Veiga-Pires, C., Correia, V., Loureiro, C., Santana, P., 2008. Chronology of the sedimentary processes during the postglacial sea level rise in two estuaries of the Algarve coast, Southern Portugal. Estuar. Coast Shelf Sci. 77, 230–244.
Brooks, N., 2012. Beyond collapse: climate change and causality during the middle Holocene climatic transition, 6400-5000 years before present. Geogr. Tidsskr. 112, 93–104.
Burjachs, F., Jones, S.E., Giralt, S., Fernández-López de Pablo, J., 2016. Lateglacial to Early Holocene recursive aridity events in the SE Mediterranean Iberian Peninsula: the Salines playa lake case study. Quat. Int. 403, 187–200. https://doi.org/10.1016/j.quaint.2015.10.117.
Cacho, I., Grimalt, J.O., Canals, M., 2002. Response of the Western Mediterranean Sea to rapid climatic variability during the last 50,000 years: a molecular biomarker approach. J. Mar. Syst. 33–34, 253–272.
Carrión, J.S., 2001. Dialectic with climatic interpretations of Late-Quaternary vegetation history in Mediterranean Spain. J. Mediterr. Ecol. 2, 145–156.
Carrión, J.S., 2002. Patterns and processes of Late Quaternary environmental change in a montane region of southwestern Europe. Quat. Sci. Rev. 21, 2047–2066.
Carrión, J.S., Andrade, A., Bennett, K.D., Navarro, C., Munuera, M., 2001. Crossing forest thresholds: inertia and collapse in a Holocene sequence from south-central Spain. Holocene 11, 635–653.
Carrión, J.S., Sánchez-Gómez, P., Mota, J.F., Yll, R., Chaín, C., Carrión, J.S., Sánchez-Gómez, P., Mota, J.F., Yll, R., Chaín, C., 2003. Holocene vegetation dynamics , fire and grazing in the Sierra de Gádor, southern Spain. Holocene 13, 839–849.
Carrión, J.S., Fernández, S., González-Sampériz, P., Leroy, S. a. G., Bailey, G., López-Sáez, J. a., Burjachs, F., Gil-Romera, G., García-Antón, M., Gil-García, M.J., Parra, I., Santos, L., López-García, P., Yll, E.I., Dupré, M., 2009. Quaternary pollen analysis in the Iberian Peninsula : the value of negative results. Internet Archaeol. 25, 1–54.
Carrión, J.S., Fernández, S., González-Sampériz, P., Gil-Romera, G., Badal, E., Carrión-Marco, Y., López-Merino, L., López-Sáez, J. a., Fierro, E., Burjachs, F., 2010. Expected trends and surprises in the lateglacial and Holocene vegetation history of the Iberian Peninsula and Balearic Islands. Rev. Palaeobot. Palynol. 162, 458–475.
Coelho, A.A., 2003. Indexing of powder diffraction patterns by iterative use of singular value decomposition. J. Appl. Crystallogr. 36, 86–95.
Cohen, A.S., 2003. Paleolimnology - the History and Evolution of Lake Systems. Oxford University Press.
Combourieu Nebout, N., Paterne, M., Turon, J.L., Siani, G., 1998. A high-resolution record of the last deglaciation in the Central Mediterranean sea: palaeovegetation and palaeohydrological evolution. Quat. Sci. Rev. 17, 303–317.
Combourieu Nebout, N., Turon, J.L., Zahn, R., Capotondi, L., Londeix, L., Pahnke, K., 2002. Enhanced aridity and atmospheric high-pressure stability over the western Mediterranean during the North Atlantic cold events of the past 50 k.y. Geology 30, 863–866.
Combourieu Nebout, N., Peyron, O., Dormoy, I., 2009. Rapid climatic variability in the west Mediterranean during the last 25 000 years from high resolution pollen data. Clim. Past Discuss 5, 671–707.
Corella, J.P., Moreno, A., Morellón, M., Rull, V., Giralt, S., Rico, M.T., Pérez-Sanz, A., Valero-Garcés, B.L., 2010. Climate and human impact on a meromictic lake during the last 6,000 years (Montcortès Lake, Central Pyrenees, Spain). J. Paleolimnol. 46, 351–367.
Cortés-Sánchez, M., Morales-Muñiz, A., Simón-Vallejo, M.D., Bergadà-Zapata, M.M., Delgado-Huertas, A., López-García, P., López-Sáez, J.A., Lozano-Francisco, M.C., Riquelme-Cantal, J.A., Roselló-Izquierdo, E., Sánchez-Marco, A., Vera-Peláez, J.L., 2008. Palaeoenvironmental and cultural dynamics of the coast of málaga (Andalusia, Spain) during the upper Pleistocene and early Holocene. Quat. Sci. Rev. 27, 2176–2193.
Davis, M.B., 1968. Pollen grains in lake sediments: redeposition caused by seasonal water circulation. Science (80-.) 162, 796–799.
Davis, B.A.S., Stevenson, A.C., 2007. The 8.2 ka event and Early-Mid Holocene forests, fires and flooding in the Central Ebro Desert, NE Spain. Quat. Sci. Rev. 26, 1695–1712.
Davis, B.A.S., Brewer, S., Stevenson, A.C., Guiot, J., Allen, J., Almqvist-Jacobson, H., Ammann, B., Andreev, A.A., Argant, J., Atanassova, J., Balwierz, Z., Barnosky, C.D., Bartley, D.D., De Beaulieu, J.L., Beckett, S.C., Behre, K.E., Bennett, K.D., Berglund, B.E.B., Beug, H.J., Bezusko, L., Binka, K., Birks, H.H., Birks, H.J.B., Björck, S., Bliakhartchouk, T., Bogdel, I., Bonatti, E., Bottema, S., Bozilova, E.D.B., Bradshaw, R., Brown, A.P., Brugiapaglia, E., Carrion, J., Chernavskaya, M., Clerc, J., Clet, M., Coûteaux, M., Craig, A.J., Cserny, T., Cwynar, L.C., Dambach, K., De Valk, E.J., Digerfeldt, G., Diot, M.F., Eastwood, W., Elina, G., Filimonova, L., Filipovitch, L., Gaillard-Lemdhal, M.J., Gauthier, A., Göransson, H., Guenet, P., Gunova, V., Hall, V.A.H., Harmata, K., Hicks, S., Huckerby, E., Huntley, B., Huttunen, A., Hyvärinen, H., Ilves, E., Jacobson, G.L., Jahns, S., Jankovská, V., Jóhansen, J., Kabailiene, M., Kelly, M.G., Khomutova, V.I., Königsson, L.K., Kremenetski, C., Kremenetskii, K.V., Krisai, I., Krisai, R., Kvavadze, E., Lamb, H., Lazarova, M.A., Litt, T., Lotter, A.F., Lowe, J.J., Magyari, E., Makohonienko, M., Mamakowa, K., Mangerud, J., Mariscal, B., Markgraf, V., McKeever, Mitchell, F.J.G., Munuera, M., Nicol-Pichard, S., Noryskiewicz, B., Odgaard, B.V., Panova, N.K., Pantaleon-Cano, J., Paus, A.A., Pavel, T., Peglar, S.M., Penalba, M.C., Pennington, W., Perez-Obiol, R., Pushenko, M., Ralska-Jasiewiszowa, M., Ramfjord, H., Regnell, J., Rybnickova, E., Rybnickova, M., Saarse, L., Sanchez Gomez, M.F., Sarmaja-Korjonen, K., Sarv, A., Seppa, H., Sivertsen, S., Smith, A.G., Spiridonova, E.A., Stancikaite, M., Stefanova, J., Stewart, D.A., Suc, J.P., Svobodova, H., Szczepanek, K., Tarasov, P., Tobolski, K., Tonkov, S.P., Turner, J., Van der Knaap, W.O., Van Leeuwen, J.F.N., Vasari, A., Vasari, Y., Verbruggen, C., Vergne, V., Veski, S., Visset, L., Vuorela, I., Wacnik, A., Walker, M.J.C., Waller, M.P., Watson, C.S., Watts, W.A., Whittington, G., Willis, K.J., Willutzki, H., Yelovicheva, Y., Yll, E.I., Zelikson, E.M., Zernitskaya, V.P., 2003. The temperature of Europe during the Holocene reconstructed from pollen data. Quat. Sci. Rev. 22, 1701–1716.
De Deckker, P., Lord, A., 2017. Cyprideis torosa : a model organism for the Ostracoda? J. Micropalaeontol. 36, 3–6. https://doi.org/10.1144/jmpaleo2016-100.
De Vicente, I., López, R., Pozo, I., Green, A.J., 2012. Nutrient and sediment dynamics in a Mediterranean shallow lake in southwest Spain. Limnética 31.
deMenocal, P.B., 2001. Cultural responses to climate change during the late Holocene. Science (80-.) 292, 667–673.
Dewald, A., Heinze, S., Jolie, J., Zilges, A., Dunai, T., Rethemeyer, J., Melles, M., Staubwasser, M., Kuczewski, B., Richter, J., Radtke, U., Von Blanckenburg, F., Klein, M., 2013. CologneAMS, a dedicated center for accelerator mass spectrometry in Germany. In: Nuclear Instruments and Methods in Physics Research, Section B: Beam Interactions with Materials and Atoms, pp. 18–23.
Dodd, J.R., Crisp, E.L., 1982. Non-linear variation with salinity of Sr/Ca and Mg/Ca ratios in water and aragonitic bivalve shells and implications for paleosalinity studies. Palaeogeogr. Palaeoclimatol. Palaeoecol. 38, 45–56.
Eusterhues, K., Heinrichs, H., Schneider, J., 2005. Geochemical response on redox fluctuations in Holocene lake sediments, Lake Steisslingen, Southern Germany. Chem. Geol. 222, 1–22.
Feely, H.W., Kulp, J.L., 1957. Origin of Gulf coast salt-dome sulphur deposits. Bull. Am. Assoc. Pet. Geol. 41, 1802–1853.
Fernández-Palacios, J.M., 1990. Lagunas de Cadiz (Medina y Salada). In: Bernues Sanz, M., A (Eds.), Humedales Espanoles En La Lisa Der Convenio de Ramsar. Ministerio de Agricultura. Pesca y Alimentación, Instituo Nacional para la Conservación de la Naturaleza, Madrid, pp. 9–24.
Fletcher, W.J., Sánchez Goñi, M.F., 2008. Orbital- and sub-orbital-scale climate impacts on vegetation of the western Mediterranean basin over the last 48,000 yr. Quat. Res. 70, 451–464.
Fletcher, W.J., Zielhofer, C., 2013. Fragility of western mediterranean landscapes during Holocene rapid climate changes. Catena 103, 16–29.
Fletcher, W.J., Boski, T., Moura, D., 2007. Palynological evidence for environmental and climatic change in the lower Guadiana valley, Portugal, during the last 13 000 years. Holocene 17, 481–494.
Fletcher, W.J., Sanchez Goñi, M.F., Peyron, O., Dormoy, I., 2010. Abrupt climate changes of the last deglaciation detected in a western Mediterranean forest record. Clim. Past 6, 245–264.
Fritz, S.C., 1996. Paleolimnological records of climatic change in North America. Limnol. Oceanogr. 41, 882–889.
Fritz, S.C., Anderson, N.J., 2013. The relative influences of climate and catchment processes on Holocene lake development in glaciated regions. J. Paleolimnol. 49, 349–362.
Giorgi, F., Lionello, P., 2008. Climate change projections for the Mediterranean region. Global Planet. Change 63, 90–104.
Giralt, S., Juliá, R., 2003. Water level reconstruction in closed lakes based on the mineral composition of sediments. In: Limnogeology in Spain: a Tribute to Kerry R. Kelts, pp. 305–325.
Glais, A., Lespez, L., Vannière, B., López-Sáez, J.A., 2017. Human-shaped landscape history in NE Greece. A palaeoenvironmental perspective. J. Archaeol. Sci. Reports 15, 405–422.
Guy-Ohlson, D., 1992. Botryococcus as an aid in the interpretation of palaeoenvironment and depositional processes. Rev. Palaeobot. Palynol. 71.
Hammer, Ø., Harper, D.A.T., Ryan, P.D., 2001. Paleontological statistics software: package for education and data analysis. Palaeontol. Electron. 1, 9–18.
Hardie, L.A., Smoot, J.P., Eugster, H.P., 1978. Saline lakes and their deposits: a sedimentological approach. In: Matter, A., Tucker, M.E. (Eds.), Modern and Ancient Lake Sediments. The International Association of Sedimentologists.
Höbig, N., Mediavilla, R., Gibert, L., Santisteban, J.I., Cendón, D.I., Ibañez, J., Reicherter, K., 2016. Palaeohydrological evolution and implications for palaeoclimate since the Late Glacial at Laguna de Fuente de Piedra, southern Spain. Quat. Int. 407, 29–46.
Hodell, D., Lourens, L., Crowhurst, S., Konijnendijk, T., Tjallingii, R., Jiménez-Espejo, F., Skinner, L., Tzedakis, P.C., Abrantes, F., Acton, G.D., Zarikian, C.A.A., Bahr, A., Balestra, B., Barranco, E.L., Carrara, G., Ducassou, E., Flood, R.D., José-Abel, Flores, Furota, S., Grimalt, J., Grunert, P., Hernández-Molina, J., Kim, J.K.,

Krissek, L.A., Kuroda, J., Li, B., Lofi, J., Margari, V., Martrat, B., Miller, M.D., Nanayama, F., Nishida, N., Richter, C., Rodrigues, T., Rodríguez-Tovar, F.J., Roque, A.C.F., Goñi, M.F.S., Sierro, F.J., Singh, A.D., Sloss, C.R., Stow, D.A.V., Takashimizu, Y., Tzanova, A., Voelker, A., Xuan, C., Williams, T., 2015. A reference time scale for site U1385 (shackleton site) on the SW Iberian margin. Global Planet. Change 133, 49–64. https://doi.org/10.1016/j.gloplacha.2015.07.002.

Huntley, B., 1991. How plants respond to climate change: migration rates, individualism and the consequences for plant communities. Ann. Bot. 67, 15–22 (S).

IGME, 1982. Geological Map, 1:50 000 Sheet Antequera 1023 (Madrid).

IPCC Core writing team, Pachauri, R.K., Meyer, L., 2014. Climate Change 2014 - Synthesis Report, Climate Change and Water.

Jalut, G., Amat Esteban, A., Riera I Mora, S., Fontugne, M., Mook, R., Bonnet, L., Gauquelin, T., Gauquelin, T., 1997. Holocene climatic changes in the western Mediterranean: Installation of the Mediterranean climate. Comptes Rendus l'Academie Sci.. - Ser. IIa Sci.. la Terre des Planetes 325, 327–334.

Jalut, G., Dedoubat, J.J., Fontugne, M., Otto, T., 2009. Holocene circum-Mediterranean vegetation changes: climate forcing and human impact. Quat. Int. 200, 4–18.

Jankovská, V., Komárek, J., 2000. Indicative value of Pediastrum and other coccal green algae in palaeoecology. Folia Geobot. 35, 59–82.

Jiménez-Espejo, F.J., Martínez-Ruiz, F., Finlayson, C., Paytan, A., Sakamoto, T., Ortega-Huertas, M., Finlayson, G., Iijima, K., Gallego-Torres, D., Fa, D., 2007. Climate forcing and Neanderthal extinction in Southern Iberia: insights from a multi-proxy marine record. Quat. Sci. Rev. 26, 836–852.

Jiménez-Espejo, F.J., Martinez-Ruiz, F., Rogerson, M., González-Donoso, J.M., Romero, O.E., Linares, D., Sakamoto, T., Gallego-Torres, D., Ruiz, J.L.R., Ortega-Huertas, M., Claros, J. a P., 2008. Detrital input, productivity fluctuations, and water mass circulation in the westernmost Mediterranean Sea since the Last Glacial Maximum. G-cubed 9.

Jiménez-Moreno, G., García-Alix, A., Hernández-Corbalán, M.D., Anderson, R.S., Delgado-Huertas, A., 2013. Vegetation, fire, climate and human disturbance history in the southwestern Mediterranean area during the late Holocene. Quat. Res. 79, 110–122.

Jiménez-Moreno, G., Rodríguez-Ramírez, A., Pérez-Asensio, J.N., Carrión, J.S., López-Sáez, J.A., Villarías-Robles, J.J., Celestino-Pérez, S., Cerrillo-Cuenca, E., Lon, A., Contreras, C., 2015. Impact of late-Holocene aridification trend, climate variability and geodynamic control on the environment from a coastal area in SW Spain. Holocene 25, 607–617.

Kaland, P.E., Krzywinsky, K., Stabell, B., 1984. Radiocarbon-dating of transitions between marine and lacustrine sediments and their relation to the development of lakes. Boreas 13, 243–258.

Lane, C.S., Brauer, A., Blockley, S.P.E., Dulski, P., 2013. Volcanic ash reveals time-transgressive abrupt climate change during the Younger Dryas. Geology 41, 1251–1254.

Langgut, D., Neumann, F.H., Stein, M., Wagner, A., Kagan, E.J., Boaretto, E., Finkelstein, I., 2014. Dead sea pollen record and history of human activity in the Judean Highlands (Israel) from the intermediate Bronze into the iron ages (~2500-500 BCE). Palynology 38, 280–302.

Laskar, J., Robutel, P., Joutel, F., Gastineau, M., Correia, A.C.M., Levrard, B., 2004. A long-term numerical solution for the insolation quantities of the Earth. Astron. Astrophys. 428, 261–285.

Lehman, J.T., 1975. Reconstructing the rate of accumulation the effect of sediment of lake Sediment : focusing '. Quat. Res. 550, 541–550.

Lillios, K.T., Blanco-González, A., Drake, B.L., López-Sáez, J.A., 2016. Mid-late Holocene climate, demography, and cultural dynamics in Iberia: a multi-proxy approach. Quat. Sci. Rev. 135, 138–153.

Lindtke, J., Ziegenbalg, S.B., Brunner, B., Rouchy, J.M., Pierre, C., Peckmann, J., 2011. Authigenesis of native sulphur and dolomite in a lacustrine evaporitic setting (Hellín basin, Late Miocene, SE Spain). Geol. Mag. 148, 655–669.

Linstädter, A., Zielhofer, C., 2010. Regional fire history shows abrupt responses of Mediterranean ecosystems to centennial-scale climate change (Olea-Pistacia woodlands, NE Morocco). J. Arid Environ. 74, 101–110.

Lionello, P., Malanotte-Rizzoli, P., Boscolo, R., Alpert, P., Artale, V., Li, L., Luterbacher, J., May, W., Trigo, R., Tsimplis, M., Ulbrich, U., Xoplaki, E., 2006. The mediterranean Climate : an overview of the main characteristics and Issues. In: Mediterranean Climate Variability, pp. 1–26.

Lopez de Pablo, J.F., Jochim, M.A., 2010. The impact of the 8,200 cal. BP climate event on human mobility srategies during the Iberian late mesolithic. J. Anthropol. Res. 66, 39–68.

Lopez, P., Navarro, E., Marce, R., Ordoñez, J., Caputo, L., Armengol, J., 2006. Elemental ratios in sediments as indicators of ecological processes in Spanish reservoirs. Limnética 25, 499–512.

López-Merino, L., López-Sáez, J.A., Alba-Sánchez, F., Pérez-Díaz, S., Carrión, J.S., 2009. 2000 years of pastoralism and fire shaping high-altitude vegetation of Sierra de Gredos in central Spain. Rev. Palaeobot. Palynol. 158, 42–51.

López-Sáez, J., López-Merino, L., 2007. Coprophilous fungi as a source of information of anthropic activities during the Prehistory in the Amblés Valley (Ávila, Spain): the archaeopalynological record. Rev. Espanola Micropaleontol. 39, 103–116.

López-Sáez, J.A., Garcıa, P.L., Sánchez, M.M., 2002. Palaeoecology and Holocene environmental change from a saline lake in South-West Spain: protohistorical and prehistorical vegetation in Cádiz Bay. Quat. Int. 93, 197–206.

López-Sáez, J.A., Blanco-González, A., López-Merino, L., Ruiz-Zapata, M.B., Dorado-Valiño, M., Pérez-Díaz, S., Valdeolmillos, A., Burjachs, F., 2009. Landscape and climatic changes during the end of the late prehistory in the amblés valley (Ávila, central Spain), from 1200 to 400 cal BC. Quat. Int. 200, 90–101.

López-Sáez, J.A., López Merino, L., Pérez Díaz, S., Alba Sánchez, F., Antonio, J., Sáez, L., Merino, L.L., Díaz, S.P., Sánchez, F.A., 2010. Paleopaisajes de Andalucía Oriental durante la transición Mesolítico-Neolítico antiguo. Os últimos caçadores-recolectores e as Prim. In: comunidades Prod. do sul da Península Ibérica e do norte Marrocos zoófilo, pp. 213–220.

López-Sáez, J.A., Abel-Schaad, D., Pérez-Díaz, S., Blanco-González, A., Alba-Sánchez, F., Dorado, M., Ruiz-Zapata, B., Gil-García, M.J., Gómez-González, C., Franco-Múgica, F., 2014. Vegetation history, climate and human impact in the Spanish Central System over the last 9000 years. Quat. Int. 353, 98–122.

Luterbacher, J., Xoplaki, E., Casty, C., Wanner, H., Pauling, A., Küttel, M., Rutishauser, T., Brönnimann, S., Fischer, E., Fleitmann, D., Gonzalez-Rouco, F.J., García-Herrera, R., Barriendos, M., Rodrigo, F., Gonzalez-Hidalgo, J.C., Saz, M.A., Gimeno, L., Ribera, P., Brunet, M., Paeth, H., Rimbu, N., Felis, T., Jacobeit, J., Dünkeloh, A., Zorita, E., Guiot, J., Türkes, M., Alcoforado, M.J., Trigo, R., Wheeler, D., Tett, S., Mann, M.E., Touchan, R., Shindell, D.T., Silenzi, S., Montagna, P., Camuffo, D., Mariotti, A., Nanni, T., Brunetti, M., Maugeri, M., Zerefos, C., Zolt, S. De, Lionello, P., Nunes, M.F., Rath, V., Beltrami, H., Garnier, E., Ladurie, E.L.R., 2006. Chapter 1 Mediterranean climate variability over the last centuries: a review. In: Developments in Earth and Environmental Sciences, pp. 27–148.

MacDonald, G.M., Beukens, R.P., Kieser, W.E., 1991. Radiocarbon dating of limnic sediments: a comparative analysis and discussion. Ecology 72, 1150–1155.

Machel, H.G., 1992. Low-temperature and high-temperature origins of elemental sulfur in diagenetic environments. In: Wessel, G.R., Wimberly, B.H. (Eds.), Native Sulfur: Developments in Geology and Exploration. Society of Mining, Metallurgy and Exploration, Littletol, Colorado, pp. 3–22.

Magny, M., Joannin, S., Galop, D., Vannière, B., Haas, J.N., Bassetti, M., Bellintani, P., Scandolari, R., Desmet, M., 2012. Holocene palaeohydrological changes in the northern Mediterranean borderlands as reflected by the lake-level record of Lake Ledro, northeastern Italy. Quat. Res. 77, 382–396.

Magri, D., Kallel, N., Narcisi, B., 2004. Palaeoenvironmental changes in the Mediterranean region 250-10 kyr BP. In: Battarbee, R.W., Gasse, F., Stickley, C.E. (Eds.), Past Climate Variability through Europe and Africa. Springer, pp. 325–342.

Martín-Puertas, C., Valero-Garces, B.L., Pilar Mata, M., Gonzalez-Samperiz, P., Bao, R., Moreno, A., Stefanova, V., Martín-Puertas, C., Valero-Garcés, B.L., Mata, M.P., González-Sampériz, P., Bao, R., Moreno, A., Stefanova, V., 2008. Arid and humid phases in southern Spain during the last 4000 years: the Zoñar Lake record, Córdoba. Holocene 18, 907–921.

Martín-Puertas, C., Valero-Garcés, B.L., Brauer, A., Mata, M.P., Delgado-Huertas, A., Dulski, P., 2009. The Iberian-roman humid period (2600-1600 cal yr BP) in the Zoñar lake varve record (Andalucía, southern Spain). Quat. Res. 71, 108–120.

Martín-Puertas, C., Jiménez-Espejo, F., Martínez-Ruiz, F., Nieto-Moreno, V., Rodrigo, M., Mata, M.P., Valero-Garcés, B.L., 2010. Late Holocene climate variability in the southwestern Mediterranean region: an integrated marine and terrestrial geochemical approach. Clim. Past 6, 807–816.

Martín-Puertas, C., Valero-Garcés, B.L., Mata, M.P., Moreno, A., Giralt, S., Martínez-Ruiz, F., Jiménez-Espejo, F., 2011. Geochemical processes in a Mediterranean Lake: a high-resolution study of the last 4,000 years in Zoñar Lake, southern Spain. J. Paleolimnol. 46, 405–421.

Mauri, A., Davis, B.A.S., Collins, P.M., Kaplan, J.O., 2015. The climate of Europe during the Holocene: a gridded pollen-based reconstruction and its multi-proxy evaluation. Quat. Sci. Rev. 112, 109–127.

Mayewski, P.A., Rohling, E.E., Stager, J.C., Karlén, W., Maasch, K.A., Meeker, L.D., Meyerson, E.A., Gasse, F., van Kreveld, S., Holmgren, K., Lee-Thorp, J., Rosqvist, G., Rack, F., Staubwasser, M., Schneider, R.R., Steig, E.J., 2004. Holocene climate variability. Quat. Res. 62, 243–255.

Medialdea, T., Somoza, L., Pinheiro, L.M., Fernández-Puga, M.C., Vázquez, J.T., León, R., Ivanov, M.K., Magalhaes, V., Díaz-del-Río, V., Vegas, R., 2009. Tectonics and mud volcano development in the Gulf of Cádiz. Mar. Geol. 261, 48–63.

Meijer, P.T., Tuenter, E., 2007. The effect precession-induced changes in the Mediterranean freshwater budget on circulation at shallow and intermediate depth. J. Mar. Syst. 68, 349–365.

Meisch, C., 2000. Freshwater Ostracoda of western and central Europe. In: Schwoerbel, J., Zwick, P. (Eds.), Freshwater Ostracoda of Western and Central Europe. Akademischer Verlag Spektrum, Heidelberg, p. 2000.

MET Office, (UKMO), Gosling, S., Dunn, R., Carrol, F., Christidis, N., Fullwood, J., de Gusmao, D., Golding, N., Good, L., Hall, T., Kendon, L., Kennedy, J., Lewis, K., McCarthy, R., McSweeney, C., Morice, C., Parker, D., Perry, M., Stott, P., Willett, K., Allen, M., Arnell, N., Bernie, D., Betts, R., Bowerman, N., Brak, B., Caesar, J., Challinor, A., Dankers, R., Hewer, F., Huntingford, C.,A.J., Klingaman, N., Lewis, K., Lloyd-Hughes, B., Lowe, J., McCarthy, R., Miller, J., Nicholls, R., Noguer, M., Otto, F., van der Linden, P., Warren, R., 2011. Climate: Observations, Projections and Impacts eprints.nottingham.as.uk/2040/.

Meyers, P.A., 1994. Preservation of elemental and isotopic source identification of sedimentary organic matter. Chem. Geol. 114, 289–302.

Meyers, P.A., 1997. Organic geochemical proxies of paleoceanographic, paleolimnologic, and paleoclimatic processes. Org. Geochem. 27, 213–250.

Meyers, P.A., 2003. Applications of organic geochemistry to paleolimnological reconstructions: a summary of examples from the Laurentian Great Lakes. Org. Geochem. 34, 261–289.

Meyers, P.A., Ishiwatari, R., 1993. Lacustrine organic geochemistry-an overview of indicators of organic matter sources and diagenesis in lake sediments. Org. Geochem. 20, 867–900.

Meyers, P.A., Lallier-Vergès, E., 1999. Lacustrine sedimentary organic matter of Late

Quaternary paleoclimates. J. Paleolimnol. 21, 345–372.
Mezquita, F., Roca, J.R., Reed, J.M., Wansard, G., 2005. Quantifying species-environment relationships in non-marine Ostracoda for ecological and palaeoecological studies: examples using Iberian data. Palaeogeogr. Palaeoclimatol. Palaeoecol. 225, 93–117.
Morellón, M., Valero-Garcés, B., Vegas-Vilarrúbia, T., González-Sampériz, P., Romero, Ó., Delgado-Huertas, A., Mata, P., Moreno, A., Rico, M., Corella, J.P., 2009. Lateglacial and Holocene palaeohydrology in the western mediterranean region: the Lake Estanya record (NE Spain). Quat. Sci. Rev. 28, 2582–2599.
Moreno, A., Pérez, A., Frigola, J., Nieto-Moreno, V., Rodrigo-Gámiz, M., Martrat, B., González-Sampériz, P., Morellón, M., Martín-Puertas, C., Corella, J.P., Belmonte, Á., Sancho, C., Cacho, I., Herrera, G., Canals, M., Grimalt, J.O., Jiménez-Espejo, F., Martínez-Ruiz, F., Vegas-Vilarrúbia, T., Valero-Garcés, B.L., 2012. The medieval climate anomaly in the Iberian Peninsula reconstructed from marine and lake records. Quat. Sci. Rev. 43, 16–32.
Nambudiri, E.M.V., Teller, J.T., Last, W.M., 1980. Pre-Quaternary microfossils—a guide to errors in radiocarbon dating. Geology 8, 123–126.
Neale, J.W., 1988. Ostracods and palaeosalinity reconstruction. In: De Dekker, P., Colin, J.-P., Peypouquet, J.P. (Eds.), Ostracoda in the Earth Sciences. Elsevier, Amsterdam, pp. 125–155.
Nieto-Moreno, V., Martínez-Ruiz, F., Giralt, S., Jiménez-Espejo, F., Gallego-Torres, D., Rodrigo-Gámiz, M., García-Orellana, J., Ortega-Huertas, M., de Lange, G.J., 2011. Tracking climate variability in the western Mediterranean during the Late Holocene: a multiproxy approach. Clim. Past 7, 1395–1414.
Olsen, J., Anderson, N.J., Knudsen, M.F., 2012. Variability of the north atlantic oscillation over the past 5,200 years. Nat. Geosci. 5, 808–812.
Ortiz, J.E., Torres, T., Delgado, A., Julià, R., Lucini, M., Llamas, F.J., Reyes, E., Soler, V., Valle, M., 2004. The palaeoenvironmental and palaeohydrological evolution of Padul Peat Bog (Granada, Spain) over one million years, from elemental, isotopic and molecular organic geochemical proxies. Org. Geochem. 35, 1243–1260.
Osborne, C.P., Mitchell, P.L., Sheehy, J.E., Woodward, F.I., 2000. Modelling the recent impacts of atmospheric CO2 and climate change on Mediterranean vegetation. Global Change Biol. 6, 445–458.
Pantaléon-Cano, J., Yll, E.-I., Pérez-Obiol, R., Roure, J.M., 2003. Palynological evidence for vegetational history in semi-arid areas of the western Mediterranean (Almería, Spain). Holocene 13, 109–119.
Peel, M.C., Finlayson, B.L., McMahon, T.A., 2007. Updated world map of the Koppen-geiger climate classification updated world map of the Köppen-Geiger climate classification. Hydrol. Earth Syst. Sci. Discuss. Eur. Geosci. Union 4 (2), 439–473.
Prentice, C., Guiot, J., Huntley, B., Jolly, D., Cheddadi, R., 1996. Reconstructing biomes from palaeoecological data: a general method and its application to European pollen data at 0 and 6 ka. Clim. Dynam. 12, 185–194. https://doi.org/10.1007/BF00211617.
Puigdefábregas, J., Mendizabal, T., 1998. Perspectives on desertification: western mediterranean. J. Arid Environ. 39, 209–224.
Quézel, P., Médail, F., 2003. Ecologie et biogégraphie des forêts du bassin méditerrannéen. Elsevier, Paris.
R Core Team, 2013. R: a Language and Environment for Statistical Computing. R Foundation for Statistical Computing, Vienna, Austria.
Ramos-Román, M.J., Jiménez-Moreno, G., Anderson, R.S., García-Alix, A., Toney, J.L., Jiménez-Espejo, F.J., Carrión, J.S., 2016. Centennial-scale vegetation and north atlantic oscillation changes during the late Holocene in the southern Iberia. Quat. Sci. Rev. 143, 84–95.
Ramos-Román, M.J., Jiménez-Moreno, G., Camuera, J., García-Alix, A., Anderson, R.S., Jiménez-Espejo, F.J., Carrión, J.S., 2018. Holocene aridification trend interrupted by millennial- and centennial-scale climate fluctuations from a new sedimentary record from Padul (Sierra Nevada, southern Iberian Peninsula). Clim. Past 14.
Ramsey, C.B., 2009. Bayesian analysis of radiocarbon dates. Radiocarbon 51, 337–360.
Rasouli, H., Scharf, B., Meisch, C., Aygen, C., 2016. An updated checklist of the Recent non-marine Ostracoda (Crustacea) of Iran, with a redescription of Eucypris mareotica (Fischer, 1855). Zootaxa 4154, 273–292.
Reed, J.M., 1996. The potential of diatoms, ostracods and other indicators for Holocene palaeoclimate research in southern Spanish salt lakes. Limnética 12, 25–39.
Reed, J.M., Stevenson, A.C., Juggins, S., 2001. A multi-proxy record of Holocene climatic change in southwestern Spain : the Laguna de Medina, Cádiz. Holocene 11, 707–719.
Reille, M., 1992. Pollen et spores d'Afrique du nord. Lab. Bot. Hist. Palynol. Marseille 9507175.
Reimer, P.J., Bard, E., Bayliss, A., Beck, J.W., Blackwell, P.G., Bronk, C., Caitlin, R., Hai, E.B., Edwards, R.L., 2013. Intcal13 and marine13 radiocarbon age calibration curves 0 – 50,000 years cal bp. Radiocarbon 55, 1869–1887.
Renaut, R.W., Gierlowski-Kordesch, E.H., 2010. Lakes. Geological Association of Canada, Toronto.
Rethemeyer, J., Fülöp, R., Höfle, S., Wacker, L., Heinze, S., Hajdas, I., Patt, U., König, S., Stapper, B., Dewald, A., 2013. Status report on sample preparation facilities for 14C analysis at the new CologneAMS center. Nucl. Instrum. Meth. Phys. Res. B 294, 168–172.
Riera Mora, S., López Sáez, J.A., Argilagós, J.B., 2004. Premieres traces d`anthropisation a l`est de la Péninsule Ibérique et les îles baléares. Ann. Littéraires 777, 195–220.
Roberts, N., Jones, M.D., Benkaddour, A., Eastwood, W.J., Filippi, M.L., Frogley, M.R., Lamb, H.F., Leng, M.J., Reed, J.M., Stein, M., Stevens, L., Valero-Garcés, B., Zanchetta, G., 2008. Stable isotope records of Late Quaternary climate and hydrology from Mediterranean lakes: the ISOMED synthesis. Quat. Sci. Rev. 27, 2426–2441.
Roca, J.R., Julià, R., 1997. Late-glacial and Holocene lacustrine evolution based on ostracod assemblages in Southeastern Spain. Geobios 30, 823–830.
Rodríguez-Rodríguez, M., Green, A.J., López, R., Martos-Rosillo, S., 2012. Changes in water level, land use, and hydrological budget in a semi-permanent playa lake, Southwest Spain. Environ. Monit. Assess. 184, 797–810.
Rodríguez-Vidal, J., Gracia, F.J., Giles, F., 1993. Deformaciones cuaternarias en la terraza fluvial de la Laguna de Medina (Río Guadalete, Jerez de la Frontera). Rev. Soc. Geol. Espana 6, 47–55.
Rudd, J.W.M., Kelly, C. a., Furutani, A., 1986. The role of sulfate reduction in longterm accumulation of organic and inorganic sulfur in lake sediments. Limnol. Oceanogr. 31, 1281–1291.
Santisteban, J.I., Mediavilla, R., Celis, A., Castaño, S., de la Losa, A., 2016. Millennial-scale cycles of aridity as a driver of human occupancy in central Spain? Quat. Int. 407, 96–109.
Schneider, H., Höfer, D., Trog, C., Mäusbacher, R., 2016. Holocene landscape development along the Portuguese Algarve coast - a high resolution palynological approach. Quat. Int. 407, 47–63.
Schröder, T., van 't Hoff, J., Ortiz, J.E., de Torres Pèrez-Hidalgo, T.J., López-Sáez, J.A., Melles, M., Holzhausen, A., Wennrich, V., Viehberg, F., Reicherter, K., 2017. Shallow hypersaline lakes as paleoclimate archives: a case study from the Laguna Salada, Málaga province, southern Spain. Quat. Int. 1–13.
Shaw, B., Mechenich, C., Klessig, L., 2004. Understanding Lake Data. Madison (Wisconsin): University of Wisconsin Cooperative Extension.
Sly, P.G., 1978. Sedimentary processes in lakes. In: Lerman, A. (Ed.), LAKES - Chemistry, Geology, Physics. Springer-Verlag Berlin Heidelberg, pp. 65–89.
Souza, P., Albuquerque Cavalcanti, I.F., 2009. Atmospheric centres of action associated wiht the Atlantic ITCZ position. Int. J. Climatol. 29, 2091–2105.
Stein, M., Starinsky, A., Katz, A., Goldstein, S.L., Machlus, M., Schramm, A., 1997. Strontium isotopic, chemical, and sedimentological evidence for the evolution of Lake Lisan and the Dead Sea. Geochem. Cosmochim. Acta 61, 3975–3992.
Swetnam, T.W., Betancourt, J.L., 1990. Fire-southern oscillation relations in the southwestern United States. Science 249, 1017–1020.
Torfstein, A., Gavrieli, I., Katz, A., Kolodny, Y., Stein, M., 2008. Gypsum as a monitor of the paleo-limnological-hydrological conditions in lake lisan and the dead sea. Geochem. Cosmochim. Acta 72, 2491–2509.
Tucker, M.E., Wright, V.P., 1990. Carbonate Sedimentology. Blackwell Publishing Ltd., Oxford, UK.
Tuenter, E., Weber, S.L., Hilgen, F.J., Lourens, L.J., 2003. The response of the African summer monsoon to remote and local forcing due to precession and obliquity. Global Planet. Change 36, 219–235.
Urban, N.R., Ernst, K., Bernasconi, S., 1999. Addition of sulfur to organic matter during early diagenesis of lake sediments. Geochem. Cosmochim. Acta 63, 837–853.
van t Hoff, J., Schröder, T., Held, P., Opitz, S., Wagner, B., Reicherter, K., Melles, M., 2016. Modern sedimentation processes in Laguna de Medina, southern Spain, derived from lake surface sediment and catchment soil samples. J. Limnol. 76, 103–115.
Valero-Garcés, B.L., González-Sampériz, P., Navas, A., Machín, J., Mata, P., Delgado-Huertas, A., Bao, R., Carrión, J.S., Schwalb, A., Gonzáles-Barrios, A., 2006. Human impact since medieval times and recent ecological restoration in a mediterranean lake the Laguna Zoñar (Spain). J. Paleolimnol. 35, 441–465.
Valero-Garcés, B., Morellón, M., Moreno, A., Corella, J.P., Martín-Puertas, C., Barreiro, F., Pérez, A., Giralt, S., Mata-Campo, M.P., 2014. Lacustrine carbonates of Iberian karst lakes: sources, processes and depositional environments. Sediment. Geol. 299, 1–29.
Vegas, J., Ruiz-Zapata, B., Ortiz, J.E., Galán, L., Torres, T., García-Cortés, Á., Gil-García, M.J., Pérez-González, A., Gallardo-Millán, J.L., 2010. Identification of arid phases during the last 50 cal. BP from the Fuentilejo maar-lacustrine record (Campo de Caltrava Volcanic Field, Spain). J. Quat. Sci. 25, 1051–1062.
Voelker, A.H.L., De Abreu, L., 2013. A review of abrupt climate change events in the northeastern Atlantic ocean (Iberian margin): latitudinal, longitudinal, and vertical gradients. Abrupt Clim. Chang. Mech. Patterns, Impacts 15–37.
Voelker, A.H.L., Lebreiro, S.M., Schönfeld, J., Cacho, I., Erlenkeuser, H., Abrantes, F., 2006. Mediterranean outflow strengthening during northern hemisphere coolings: a salt source for the glacial Atlantic? Earth Planet Sci. Lett. 245, 39–55.
Voelker, A.H.L., De Abreu, L., Schönfeld, J., Erlenkeuser, H., Abrantes, F., 2009. Hydrographic conditions along the western Iberian margin during marine isotope stage 2. G-cubed 10.
Walker, M.J.C., 2005. Quaternary Dating Methods., Quaternary Geochronology. John Wiley & Sons, Ltd.
Walker, M.J.C., Berkelhammer, M., Björck, S., Cwynar, L.C., Fisher, D.A., Long, A.J., Lowe, J.J., Newnham, R.M., Rasmussen, S.O., Weiss, H., 2012. Formal subdivision of the Holocene series/epoch: a discussion paper by a working group of intimate (Integration of ice-core, marine and terrestrial records) and the subcommission on quaternary stratigraphy (International commission on stratigraphy). J. Quat. Sci. 27, 649–659.
Wanner, H., Beer, J., Bütikofer, J., Crowley, T.J., Cubasch, U., Flückiger, J., Goosse, H., Grosjean, M., Joos, F., Kaplan, J.O., Küttel, M., Müller, S.A., Prentice, I.C., Solomina, O., Stocker, T.F., Tarasov, P., Wagner, M., Widmann, M., 2008. Mid- to Late Holocene climate change: an overview. Quat. Sci. Rev. 27, 1791–1828.
Wanner, H., Solomina, O., Grosjean, M., Ritz, S.P., Jetel, M., 2011. Structure and origin

of Holocene cold events. Quat. Sci. Rev. 30, 3109–3123.
Whelan, R.J., 1995. The Ecology of Fire. Cambridge University Press.
Wolf, D., Seim, A., Faust, D., 2014. Fluvial system response to external forcing and human impact - late Pleistocene and Holocene fluvial dynamics of the lower Guadalete River in western Andalucía (Spain). Boreas 43, 422–449.
Ziegenbalg, S.B., Brunner, B., Rouchy, J.M., Birgel, D., Pierre, C., Böttcher, M.E., Caruso, A., Immenhauser, A., Peckmann, J., 2010. Formation of secondary carbonates and native sulphur in sulphate-rich Messinian strata, Sicily. Sediment. Geol. 227, 37–50.